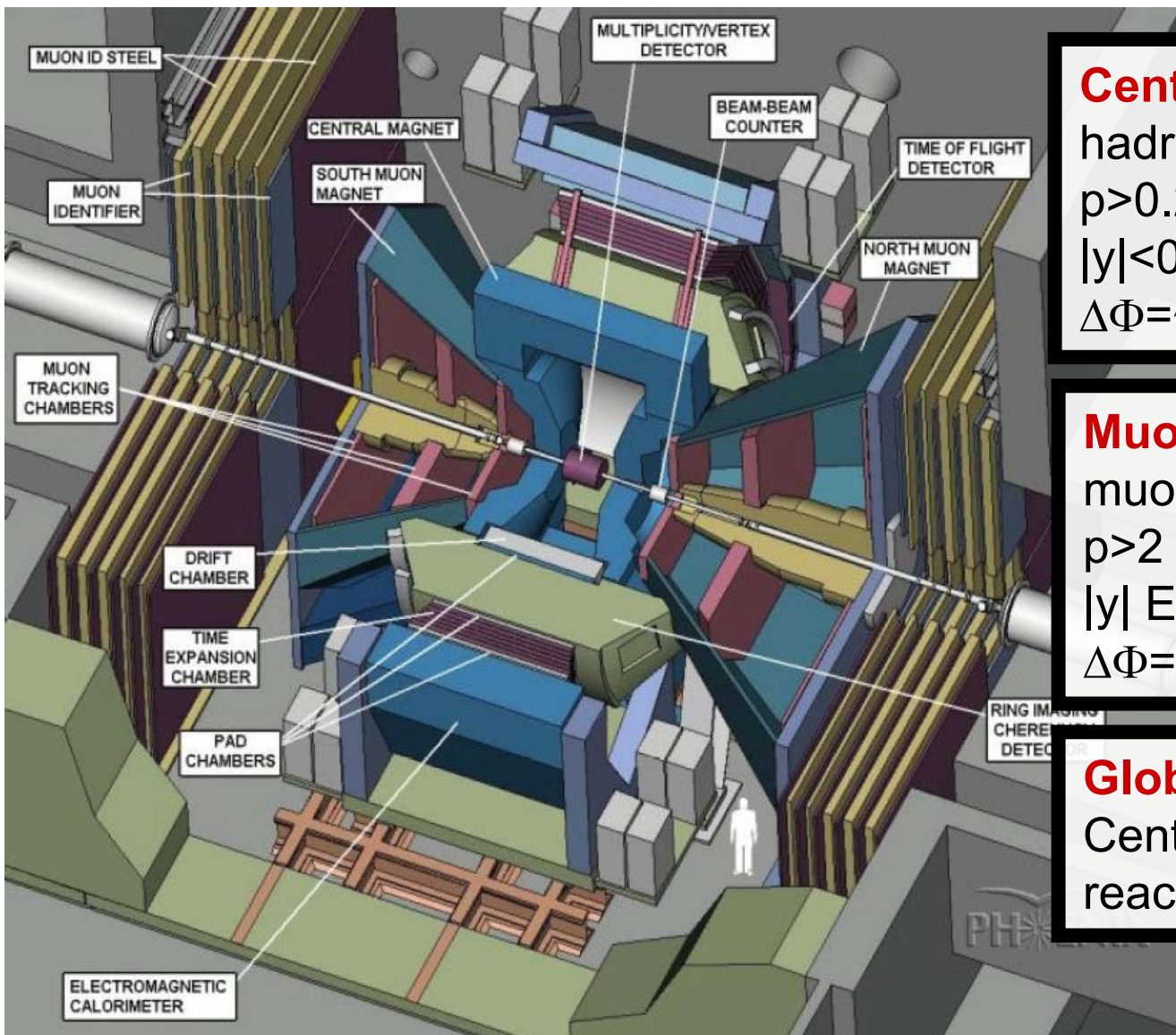


Recent results from the PHENIX experiment at RHIC

Hugo Pereira Da Costa, CEA Saclay, PHENIX collaboration
Etretat, September 18 2007

Introduction

The PHENIX detector



Central arm

hadrons; photons; electrons
 $p > 0.2 \text{ GeV}/c$
 $|y| < 0.35$
 $\Delta\Phi = \pi$

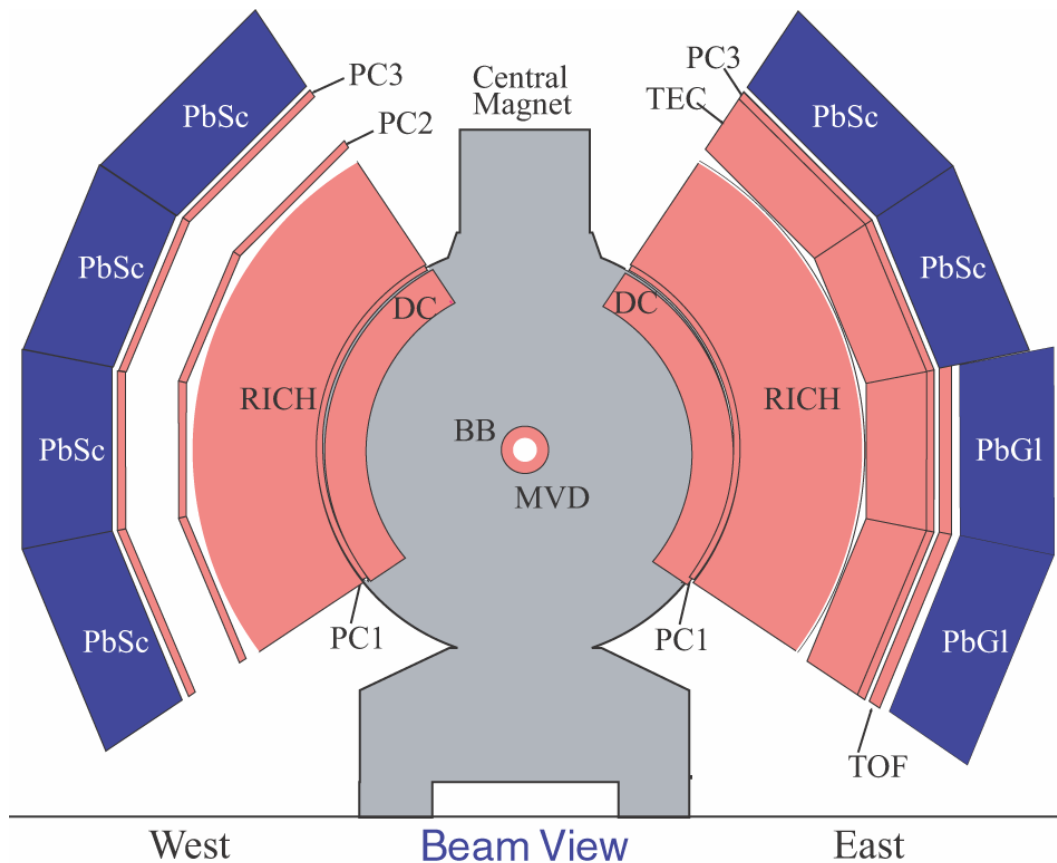
Muon arms

muons; stopped hadrons
 $p > 2 \text{ GeV}/c$
 $|y| \in [1.2, 2.4]$
 $\Delta\Phi = 2\pi$

Global detectors

Centrality, vertex position,
reaction plane

The PHENIX detector – central arms



Tracking:

Drift Chambers,
Pad Chambers,
Time Expansion Chamber

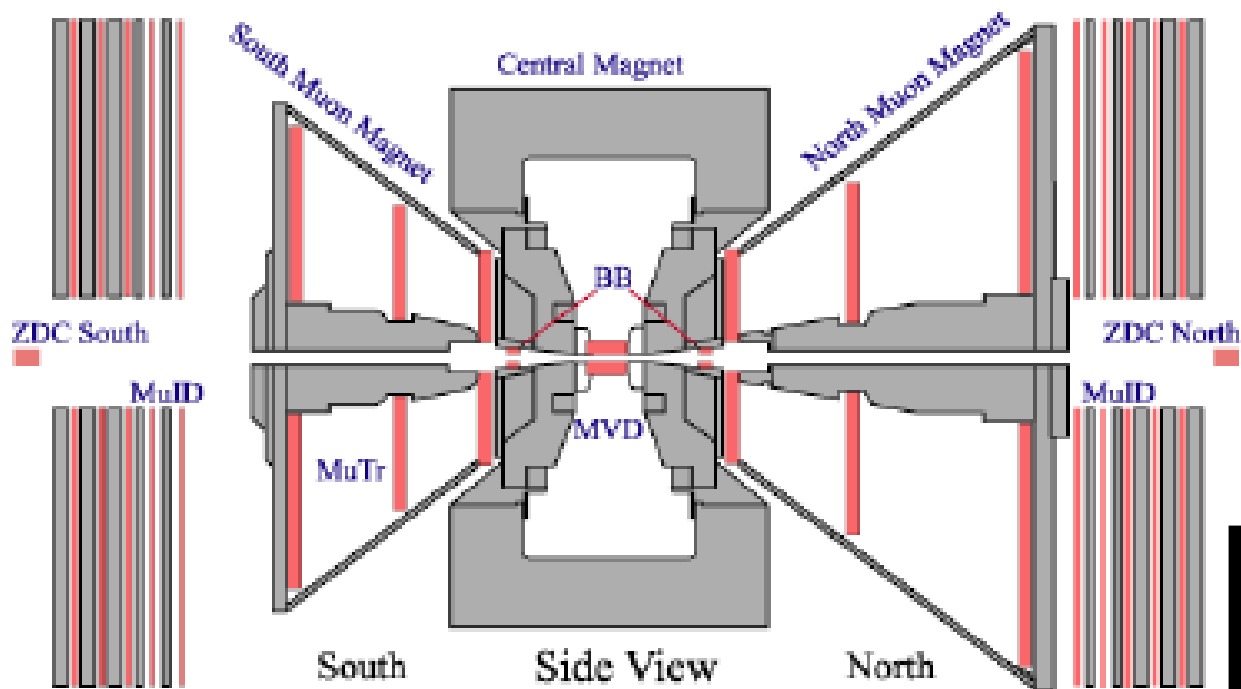
Calorimetry:

PbGl and PbSc EMCal
also used for triggering

Particle identification:

RICH
Time Of Flight

The PHENIX detector – muon arms



Front absorber to stop hadrons

Tracking:

3 muon tracker stations of cathode strip chambers with radial magnetic field

Muon identification:

5 detection planes (X and Y) and absorber, also used for triggering

PHENIX capabilities

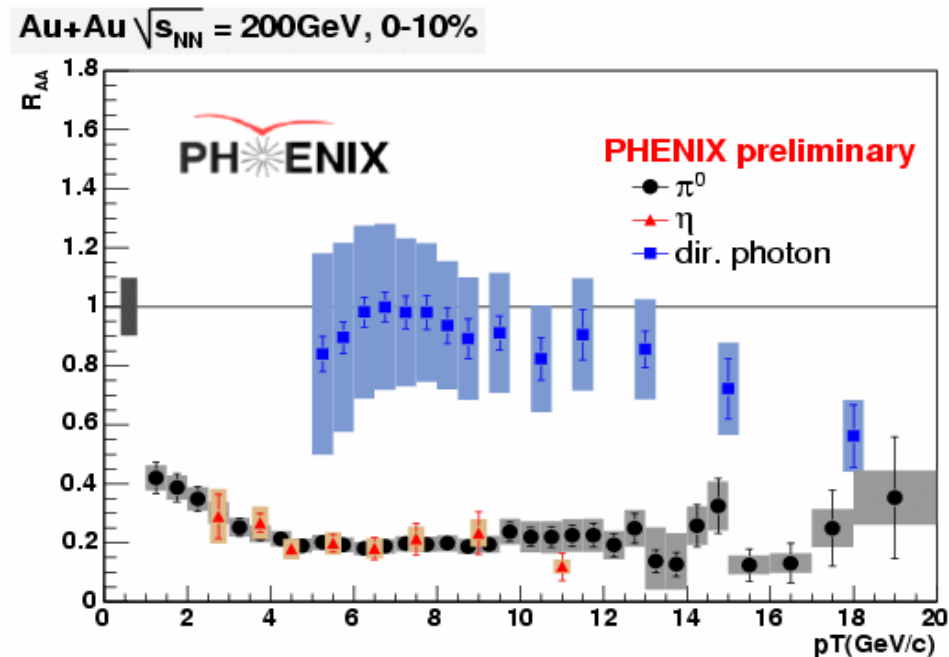
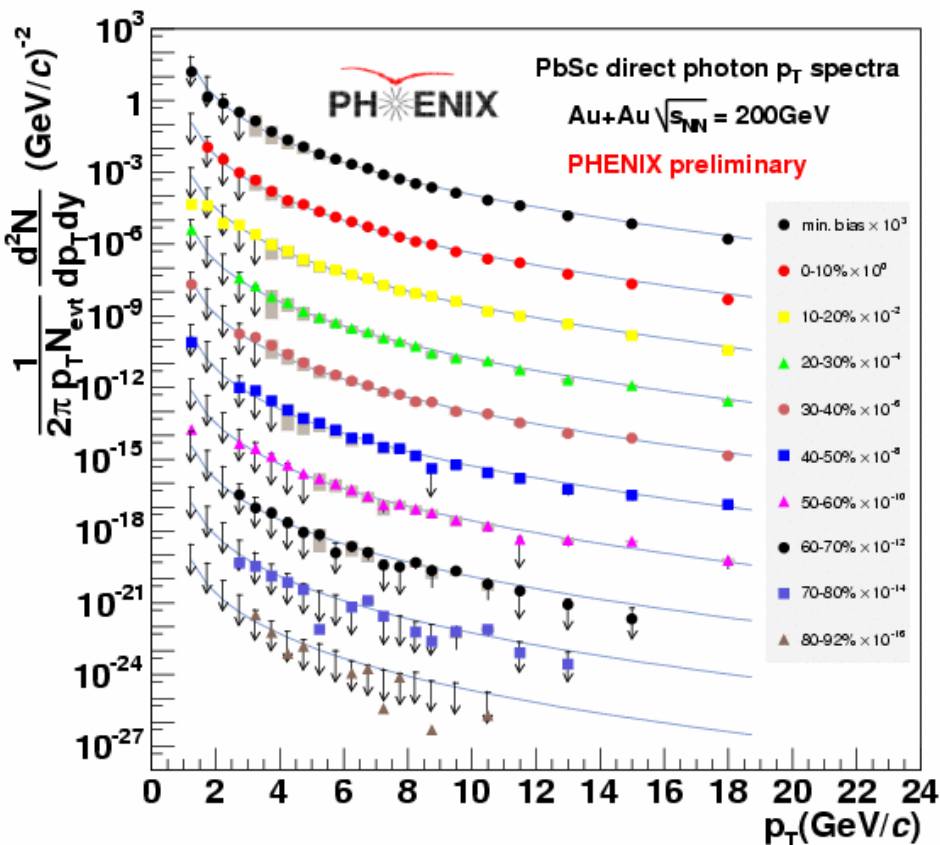
- **photons:** direct photons, π^0/η over a large p_T range (0-20 GeV/c)
- **charged hadrons** ($\pi^{+/-}$, $K^{+/-}$, etc.)
- **light meson resonances** (ϕ , ω , η) via both electromagnetic and hadronic decays
- **single leptons** (electrons/muons): heavy flavor
- **di-leptons:** heavy flavor, J/Ψ (in 2 rapidity domains)

Outline

- energy loss (direct photons and light and heavy quarks)
- elliptic flow and thermalization
- jet correlations
- di-lepton continuum and heavy quarkonia

Energy loss

direct photons, π^0 and η

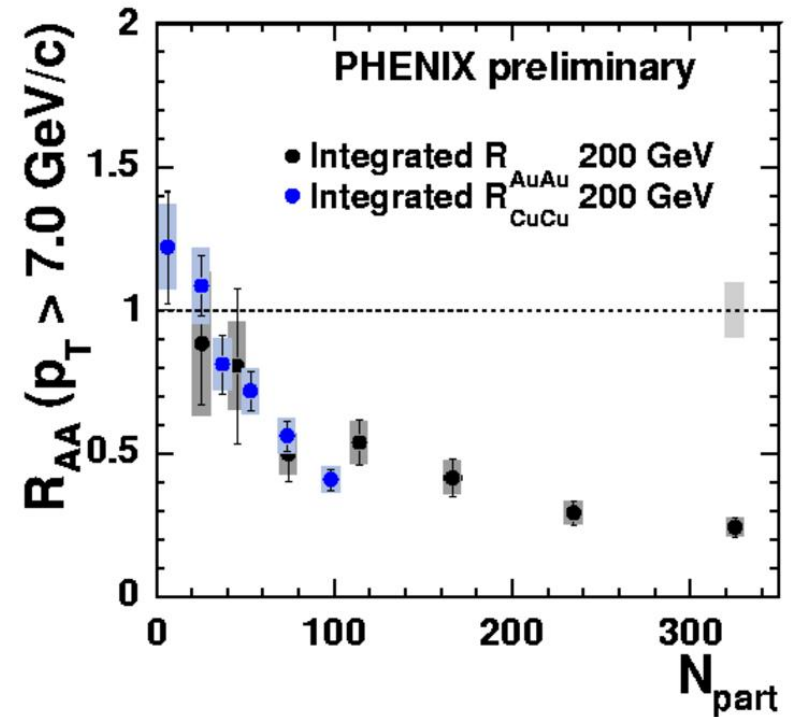
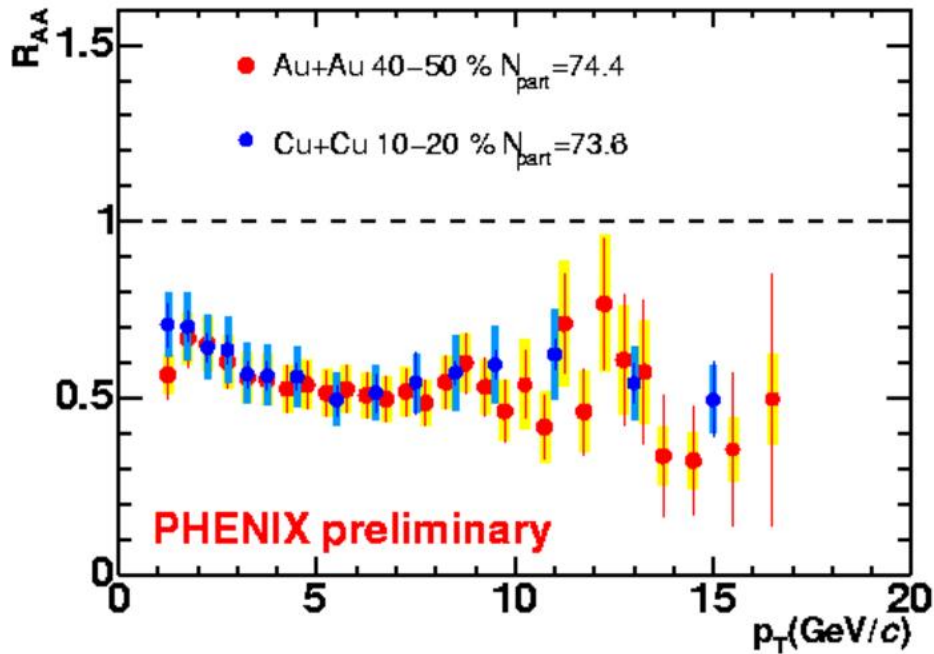


Direct photons and π^0 R_{AA} measurement extended to very high p_T

New methods at low p_T (1-4 GeV/c) for photons (not shown here)

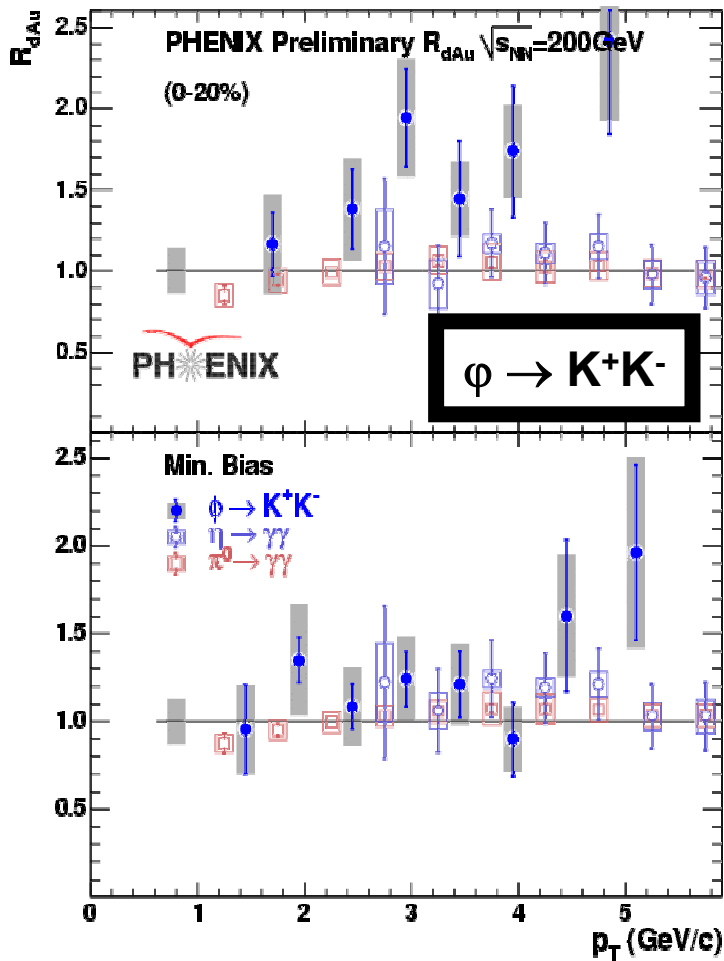
No direct photon suppression until 14 GeV
 π^0 suppression stays nearly constant up to 20 GeV/c

System size dependence of $\pi^0 R_{AA}$

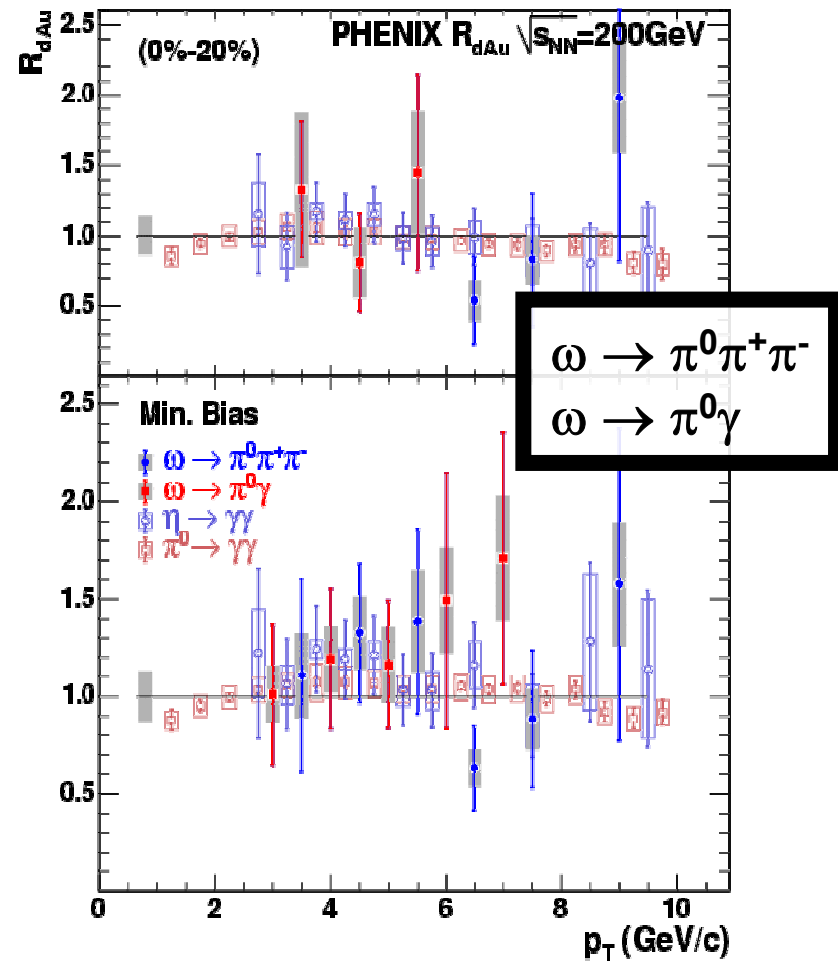


R_{AA} is the same in Cu+Cu and Au+Au at equal N_{part}

Light mesons R_{dAu}



R_{dAu} for Φ , η and π^0 vs p_T @200 GeV in 0-20% and minimum bias



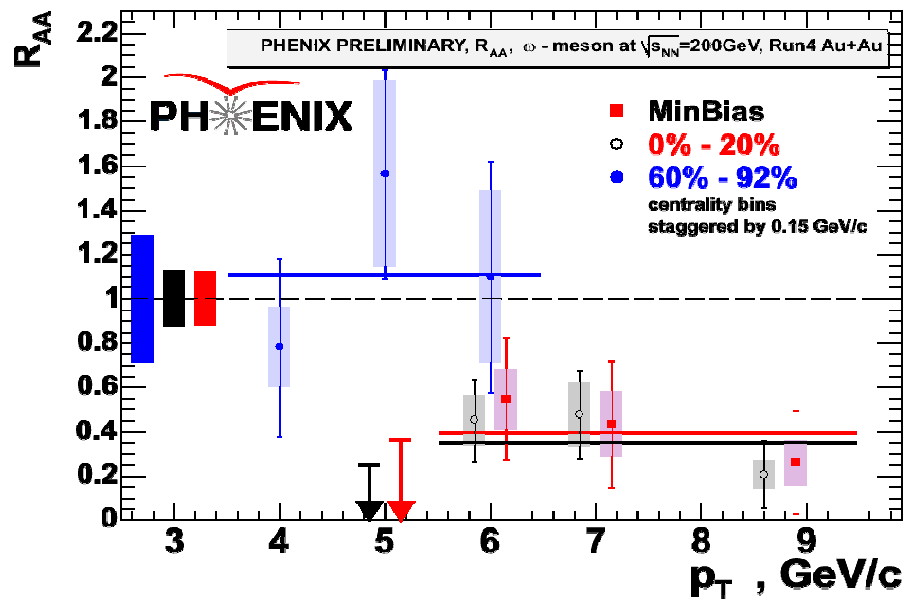
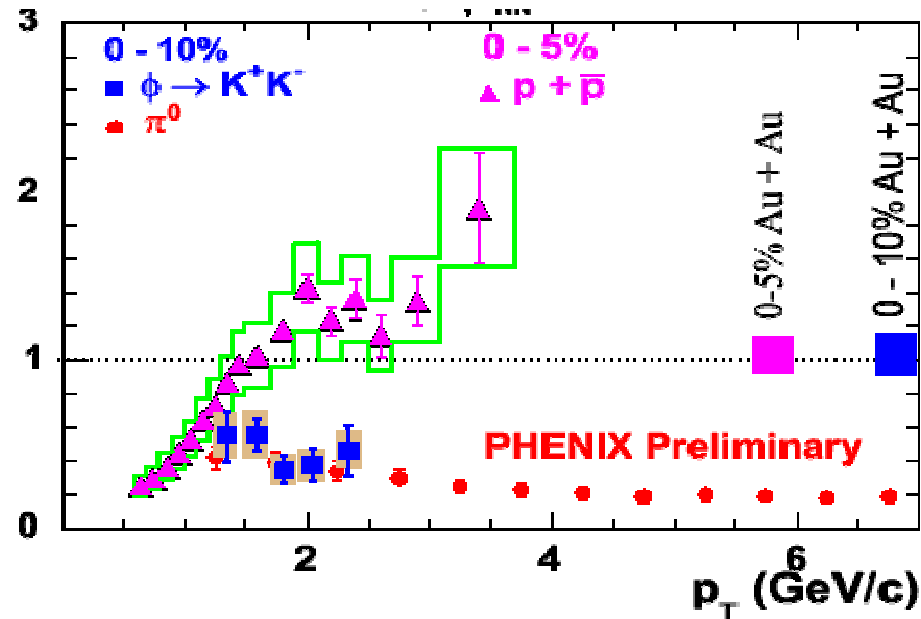
R_{dAu} for ω , η and π^0 vs p_T @200 GeV in 0-20% and minimum bias

All R_{AA} are compatible with 1.
Large error bars prevent to quantify any cold nuclear matter effect

light mesons R_{AA}

ϕ , ρ and π in Au+Au@200 GeV
0-10%

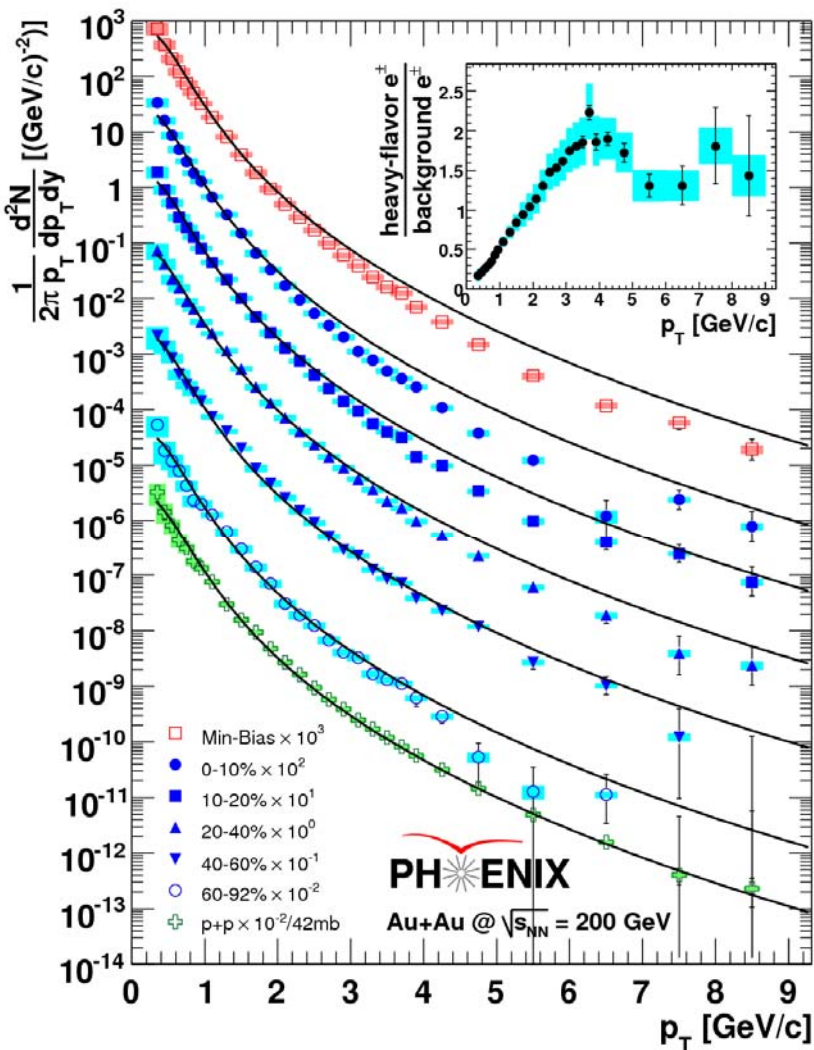
ω in Au+Au@200 GeV
60-92% and 0-20%



A high p_T suppression is observed for ϕ and ω ,
similar to that observed for π and η

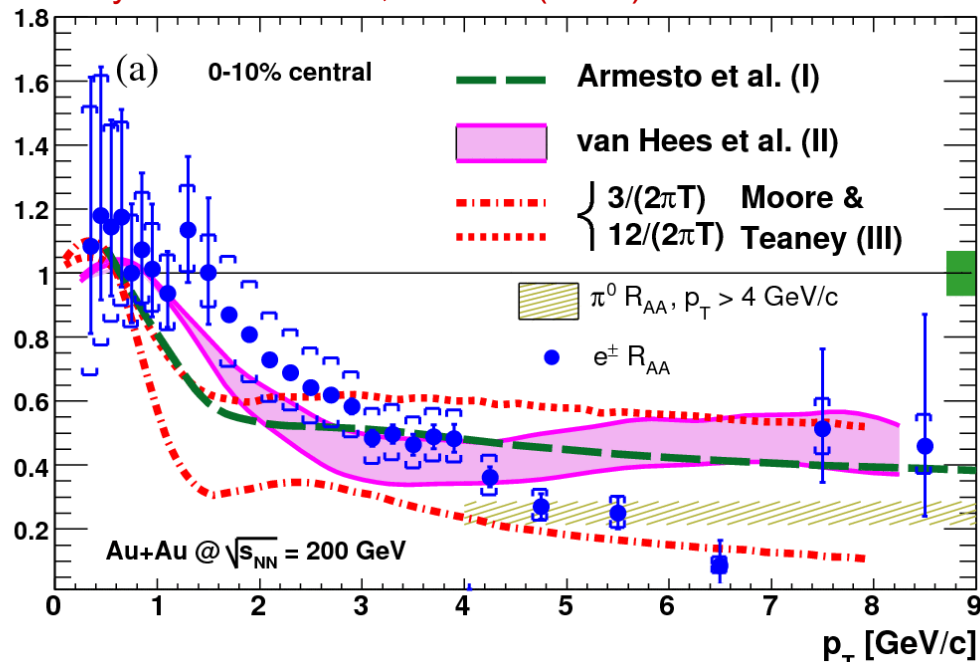
Heavy quarks

Non-photonic single electron vs centrality in Au+Au@200 GeV/c



Non-photonic electron R_{AA} vs p_T in Au+Au@200 GeV, 0-10% central

Phys. Rev. Lett. 98, 172301 (2007)



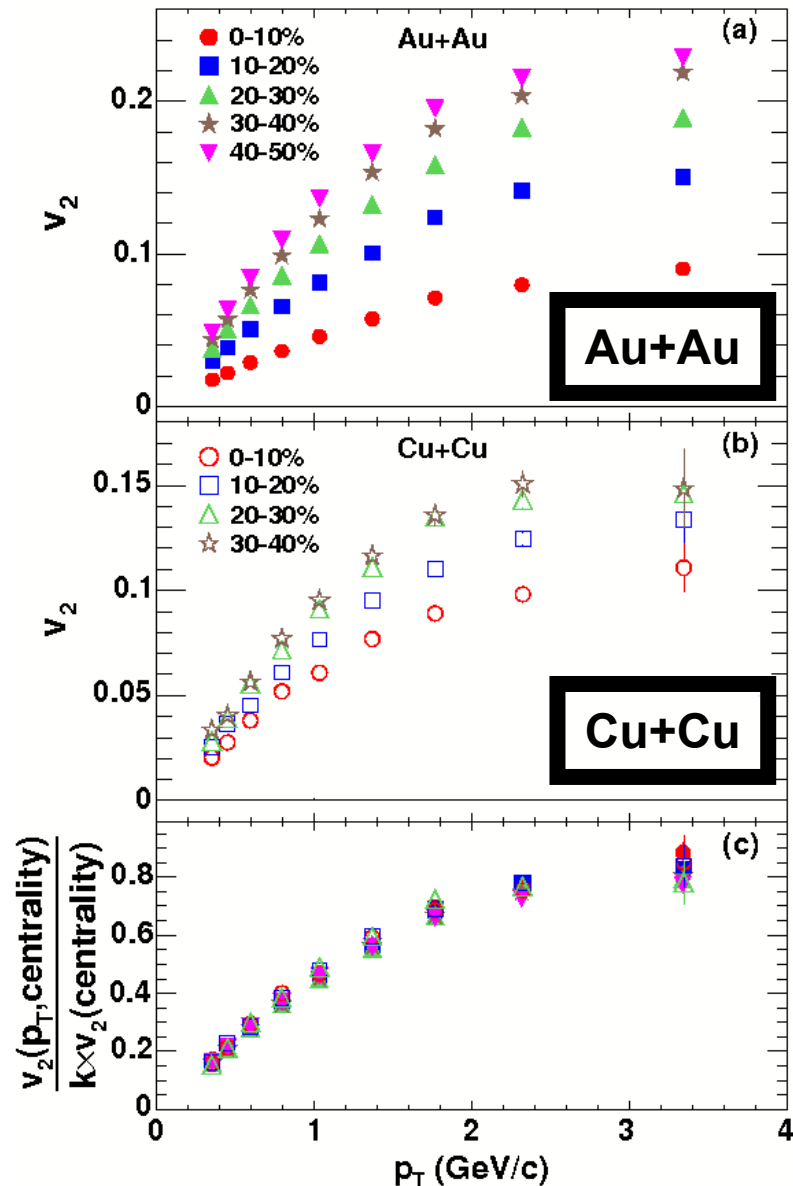
Sizeable suppression is measured.
Slightly smaller than for pions

Models aim to describe R_{AA} and v_2 simultaneously.

Elliptic flow

v_2 vs p_T , centrality and collision system

Phys. Rev Lett. 98, 162301 (2007)



The elliptic flow, v_2 characterizes the azimuthal anisotropy of the medium collective motion.

v_2 increases from central to peripheral collisions. This is expected because the eccentricity of the overlapping area increases.

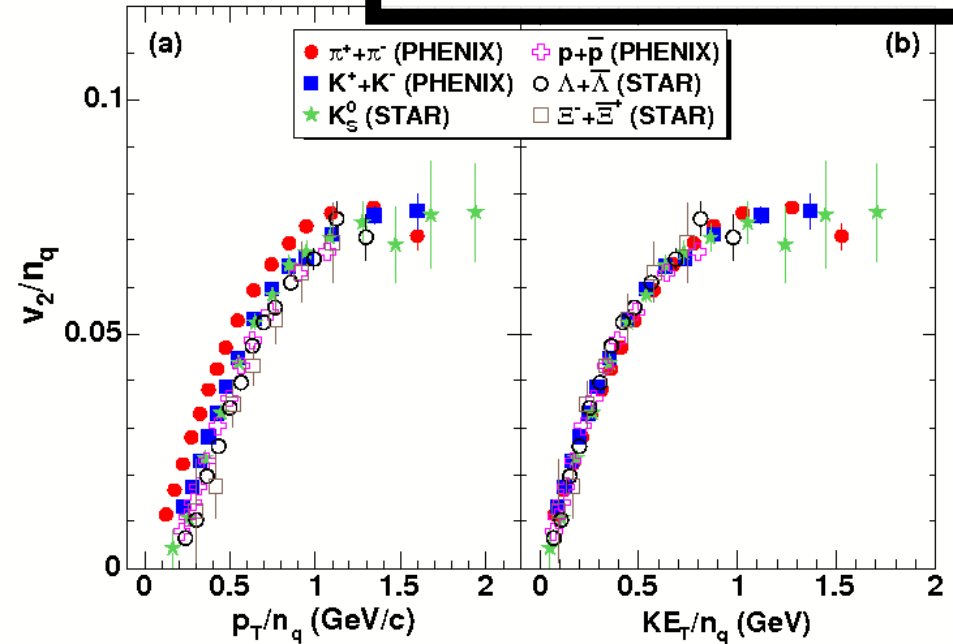
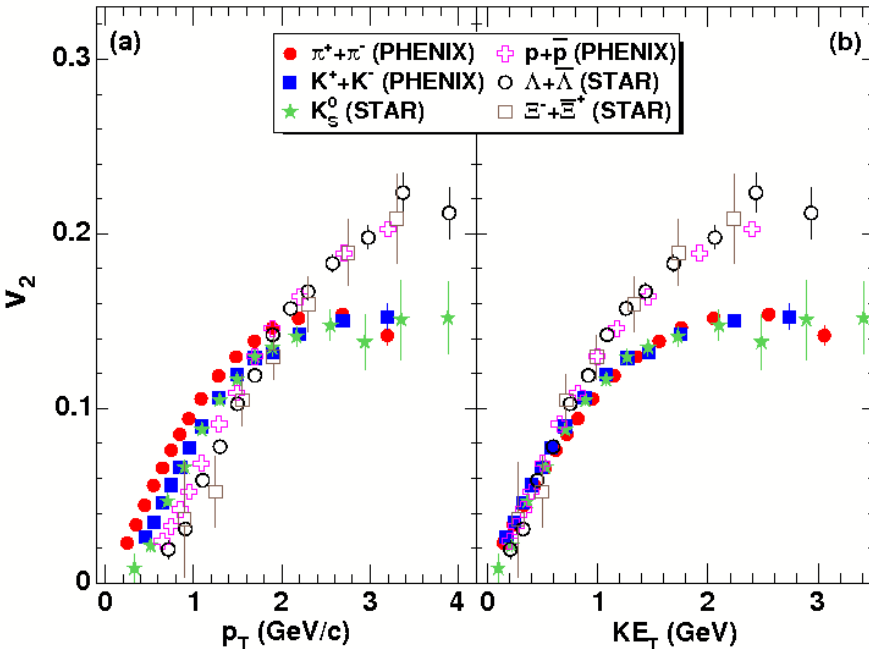
Differential v_2 normalized to its integral is universal, meaning that the measured v_2 is controlled by the geometry of the overlapping region only.

Hydrodynamic models predict that $\int v_2$ is proportional to the eccentricity.

v_2 vs p_T , KE_T and n_q

Phys. Rev Lett. 98, 162301 (2007)

Au+Au@200GeV min. bias



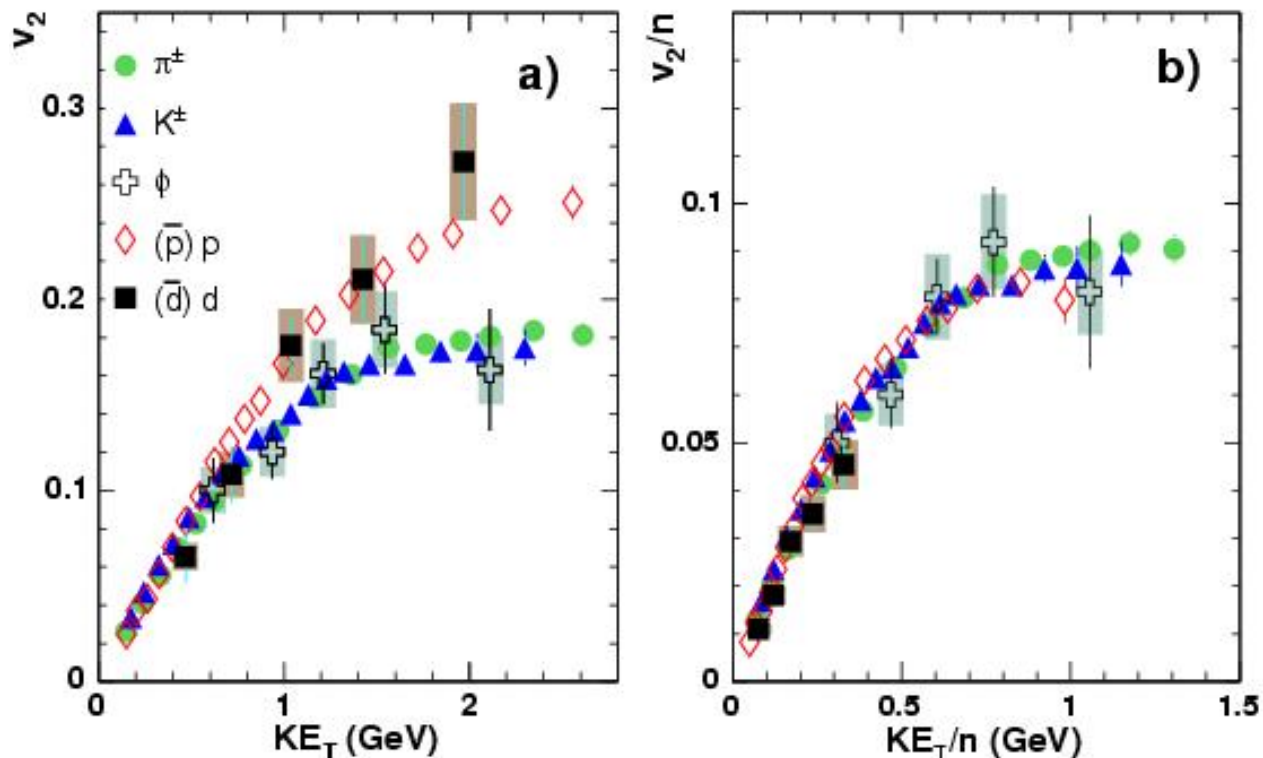
Universal scaling observed when:

- at low p_T when using the transverse kinetic energy $KE_T = m_T - m$ in place of p_T
- at high p_T when dividing both axis by the number of constituent quarks n_q

Indication that the v_2 develops at a pre-hadronic stage

ϕ , d and \bar{d}

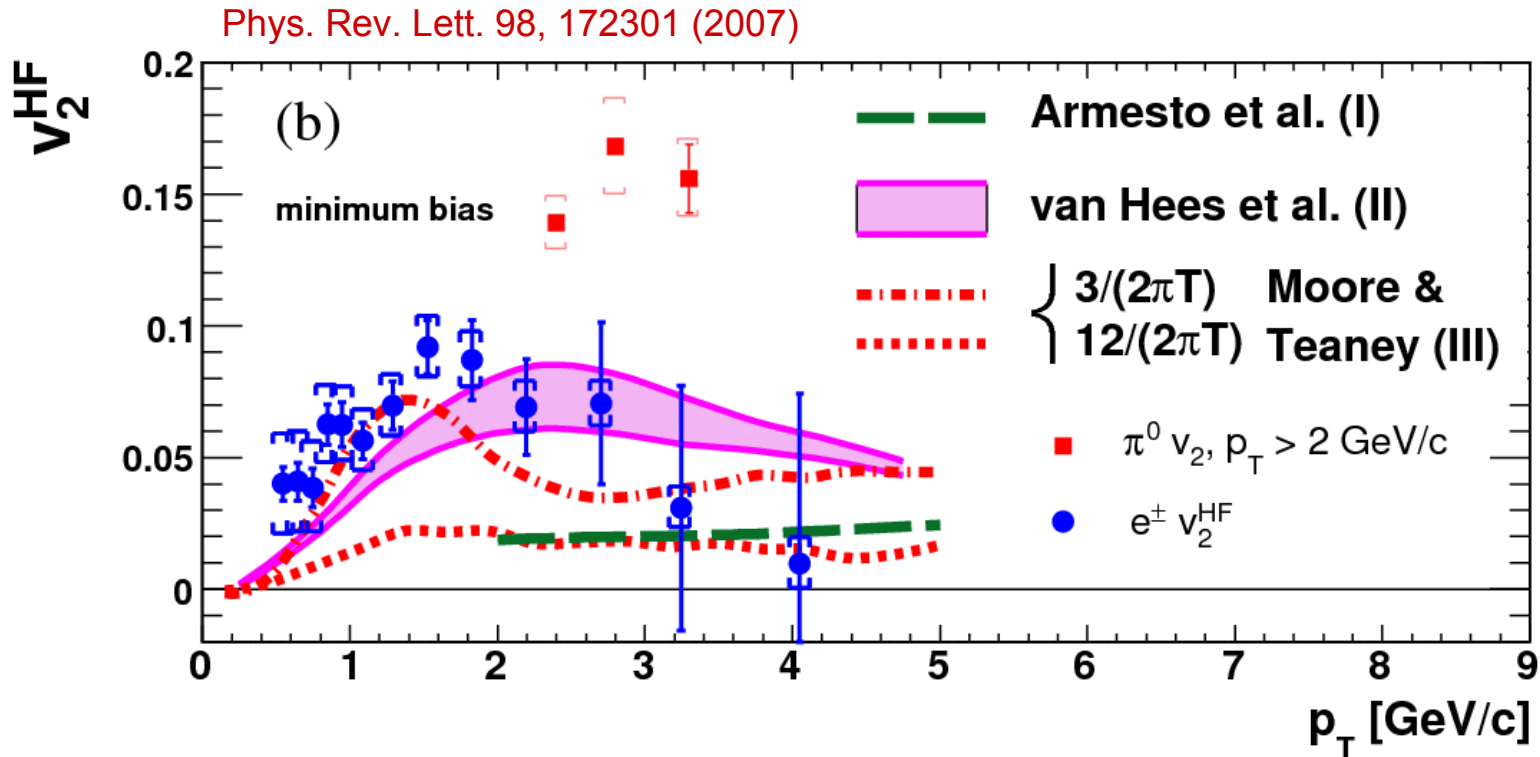
nucl-ex/0703024



- ϕ mesons have small hadronic cross-sections, but fall on the same curve.
- d and \bar{d} also follow the same trend (although in a limited KE_T/n_q range), with $n_q = 6$.

Indication that the v_2 develops at a pre-hadronic stage

Heavy quarks



Sizeable v_2 indicates strong coupling of charm to the medium.

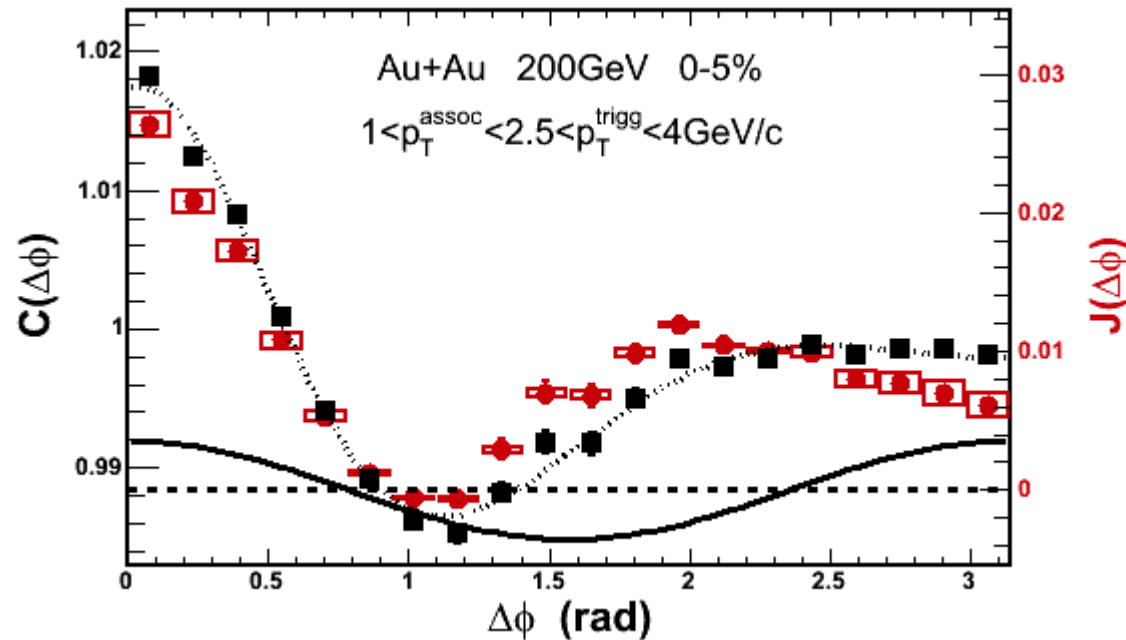
Presented calculations attempt to describe simultaneously charm R_{AA} and v_2 .

They favor small charm relaxation time in medium and small viscosity for the surrounding medium, consistent with estimates from light hadrons measurements.

Jet correlations

Jet correlations (principle)

Jet correlation functions are derived from raw azimuthal correlations between a trigger particle of high p_T and same event associate particles, divided by the acceptance using event-mixing and subtracted by the underlying event v_2 contribution.

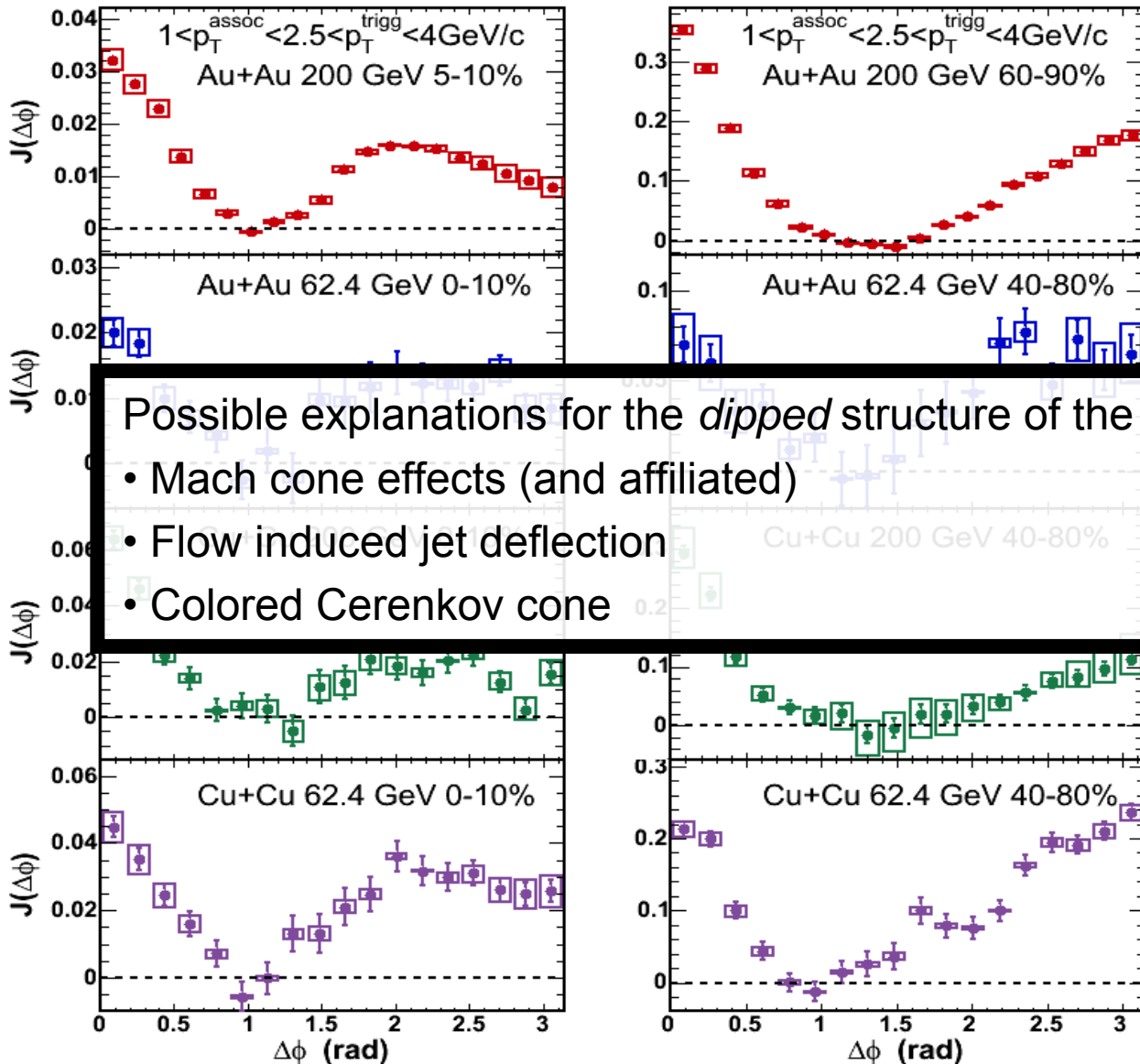


Black is acceptance corrected correlation function.

Solid line is the v_2 contribution.

Red is v_2 subtracted correlation function (using ZYAM method).

Away side jet modification vs system and energy

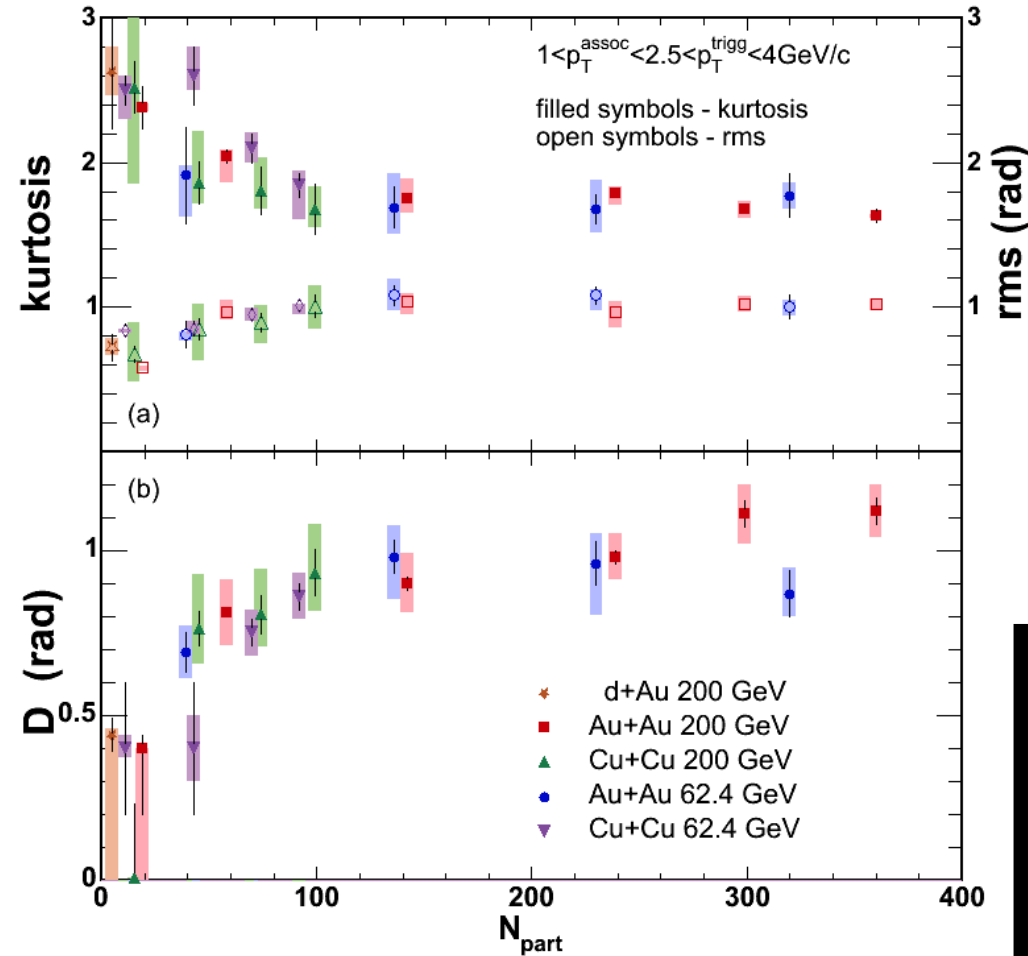


Possible explanations for the *dipped* structure of the away side jet include:

- Mach cone effects (and affiliated)
- Flow induced jet deflection
- Colored Cerenkov cone

Away side jet modifications vs system and energy

nucl-ex/0611019



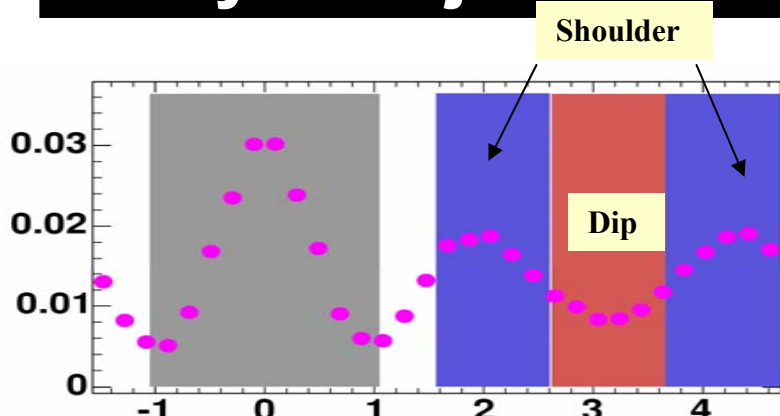
Here the shape of the away-side peak is characterized using 3 variables:

- RMS
- Kurtosis (=3 for Gaussian)
- D, distance between the peak and the local minimum, at $\Delta\phi = \pi$

The broadening and peak location are found to depend on N_{part} , but not on the collision energy or colliding nuclei.

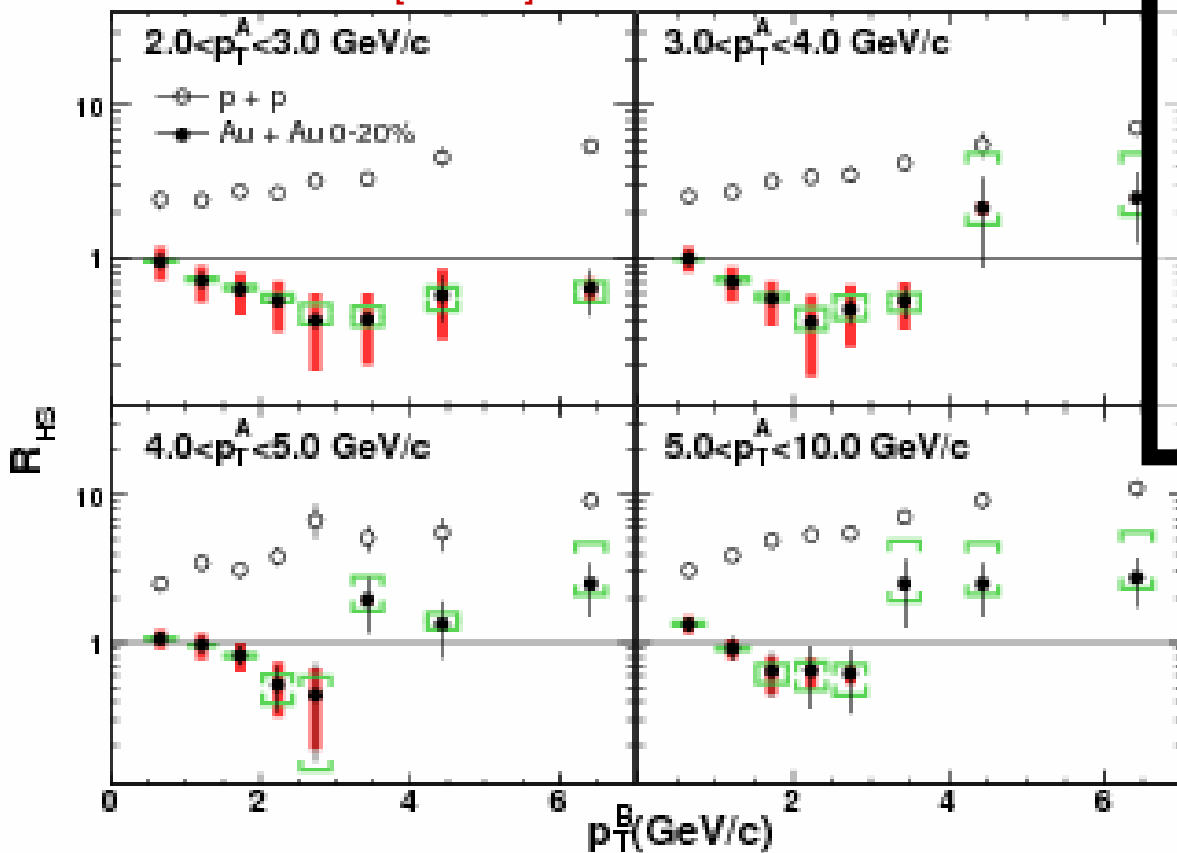
It is also independent of p_T^{assoc} (not shown here).

Away side jet modifications vs $p_T^{\text{trig}} \times p_T^{\text{assoc}}$



Here the shape of the away-side peak is characterized using the ratio R_{HS} between the integral in the *head* region over the integral in the *shoulder* region

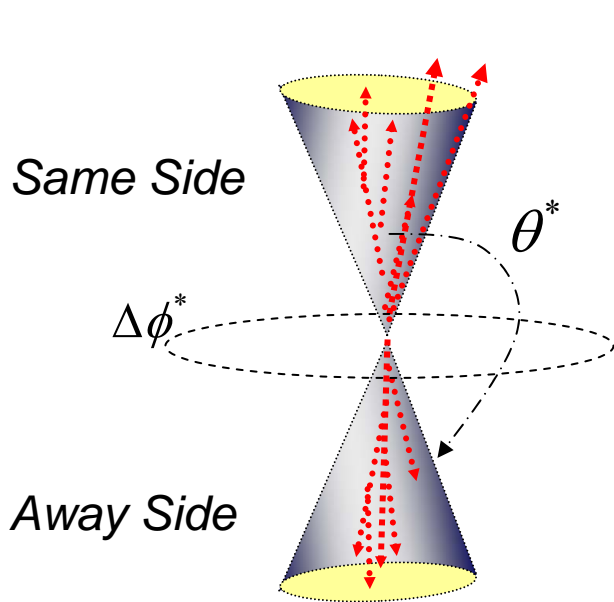
arXiv:0705.3238 [nucl-ex]



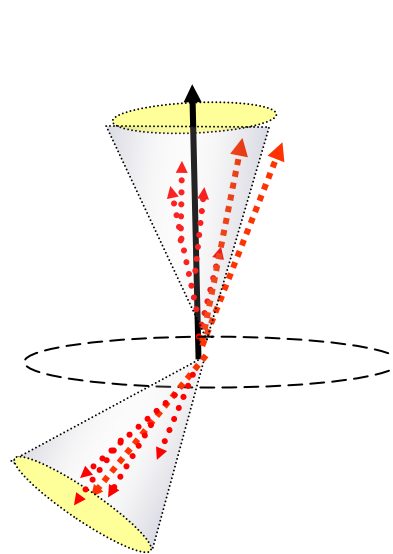
$R_{\text{HS}} < 1$ for small $P_T^A \times P_T^B$ are representative of the dip at $\Delta\phi = \pi$.

$R_{\text{HS}} > 1$ for large $P_T^A \times P_T^B$ are interpreted as a *re-appearance* of the away side peak, possibly due to *punch-through* jets

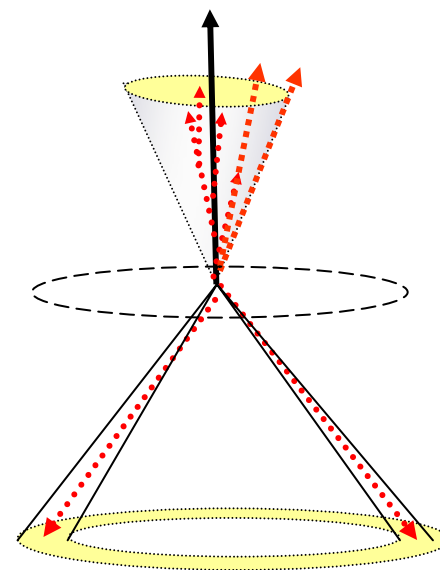
Three particles correlations (principle)



Normal jet simulations



Deflected jet simulations



Mach Cone simulations

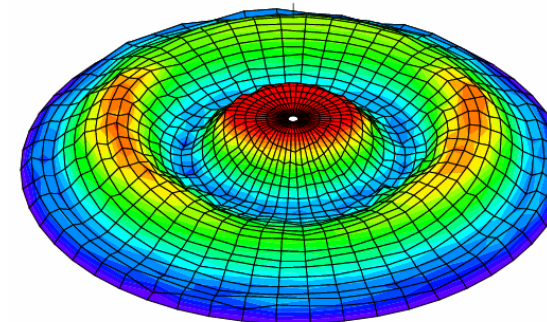
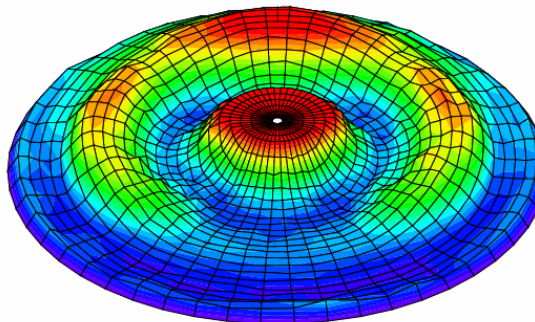
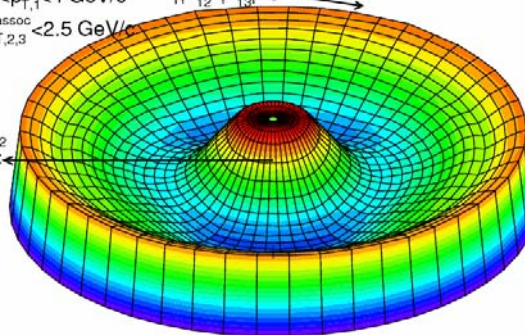
SIM Normal Jet Correlation PHENIX Acceptance

$2.5 < p_{T,1}^{\text{trig}} < 4 \text{ GeV}/c$ $|\phi_{12}^* - \phi_{13}^*| = 0$

$1 < p_{T,2,3}^{\text{assoc}} < 2.5 \text{ GeV}/c$

θ_{12}^*

$= \pi$

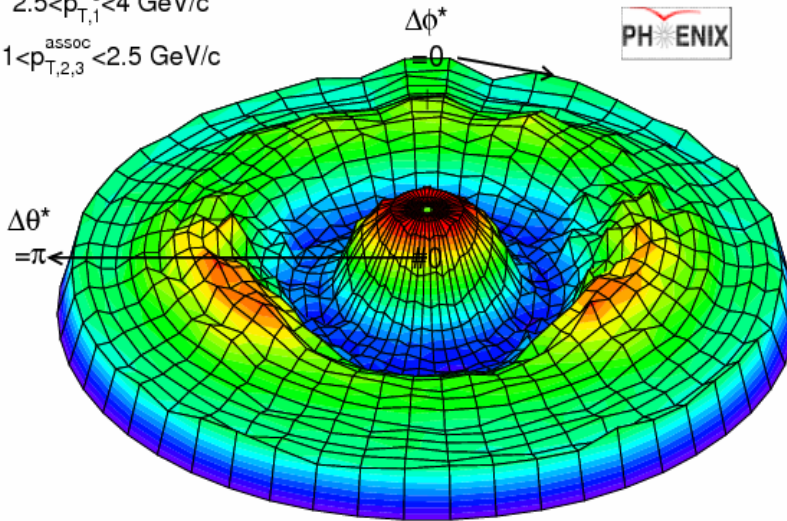


Three particles correlations (data)

$\sqrt{s_{NN}}=200\text{GeV}$ PHENIX Total 3-Particle Jet Corrln. Cent = 10-20%

$2.5 < p_{T,1}^{\text{trig}} < 4 \text{ GeV}/c$

$1 < p_{T,2,3}^{\text{assoc}} < 2.5 \text{ GeV}/c$



PHENIX Preliminary

Associate particle yield variation along $\Delta\Phi$

Blue is for deflected jets simulations

Red is for Mach cone effects

Data favor a Mach cone like structure

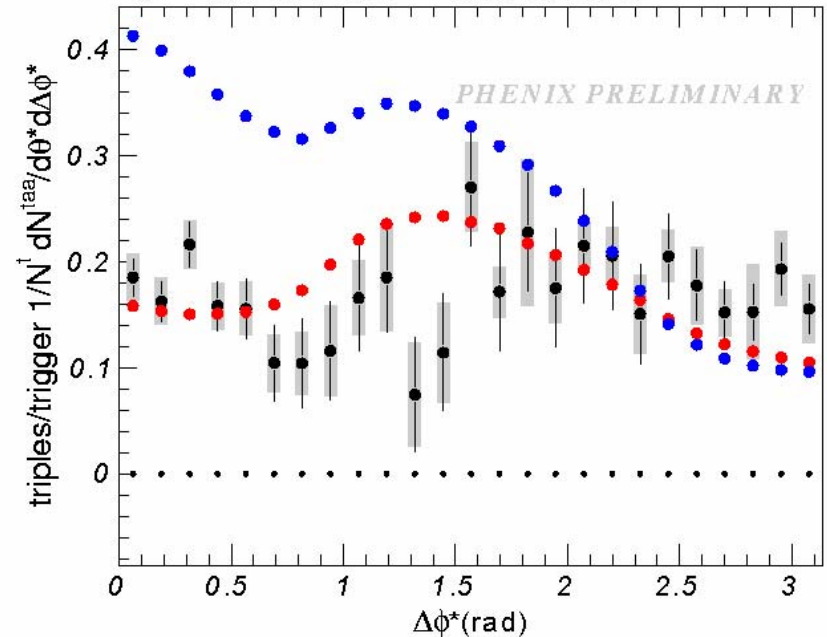


Au+Au $\sqrt{s_{NN}}=200 \text{ GeV}$

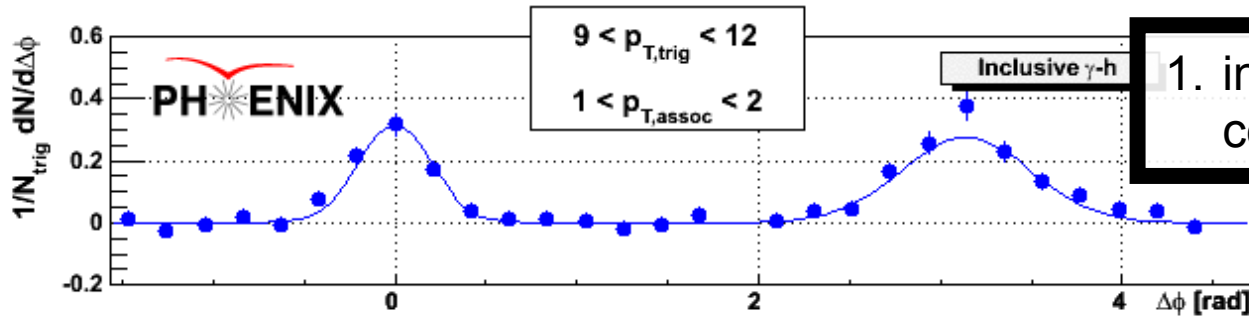
PHENIX η True 3-Particle Jet Correlation along $\Delta\phi^*$

$2.5 < p_{T,1}^{\text{trig}} < 4 \text{ GeV}/c$ $1 < p_{T,2,3}^{\text{assoc}} < 2.5 \text{ GeV}/c$

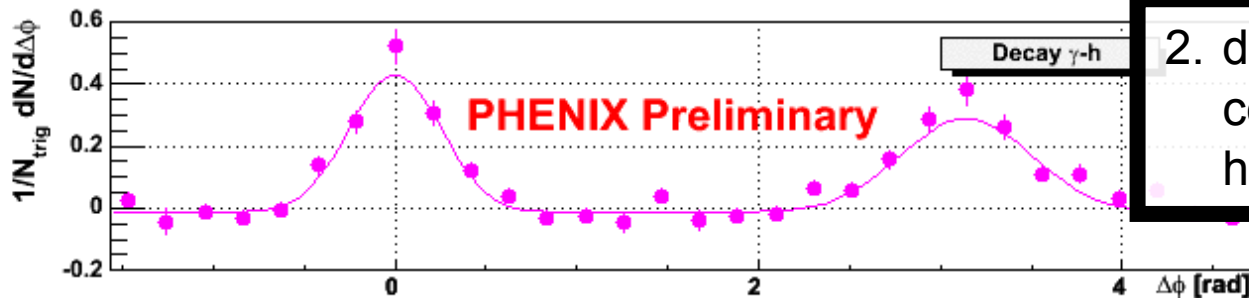
$\theta^* = \langle 1.65-2.2 \rangle \text{ rad}$ cent 10-20 %



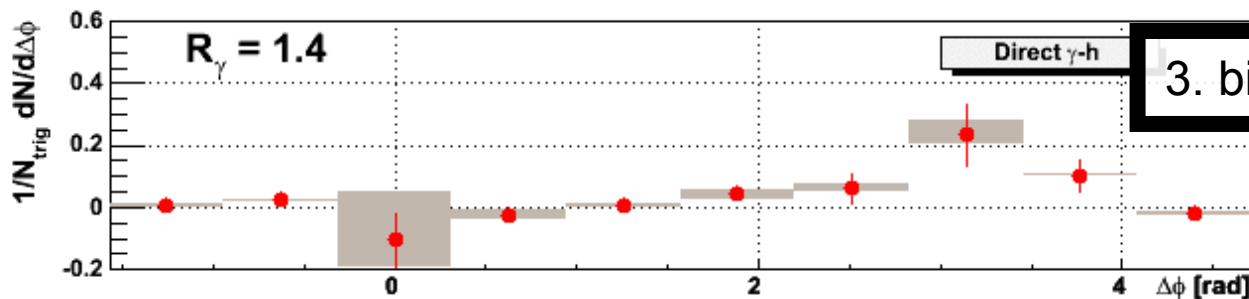
Gamma_{direct} - jet correlations (principle)



1. inclusive gamma-hadron correlations



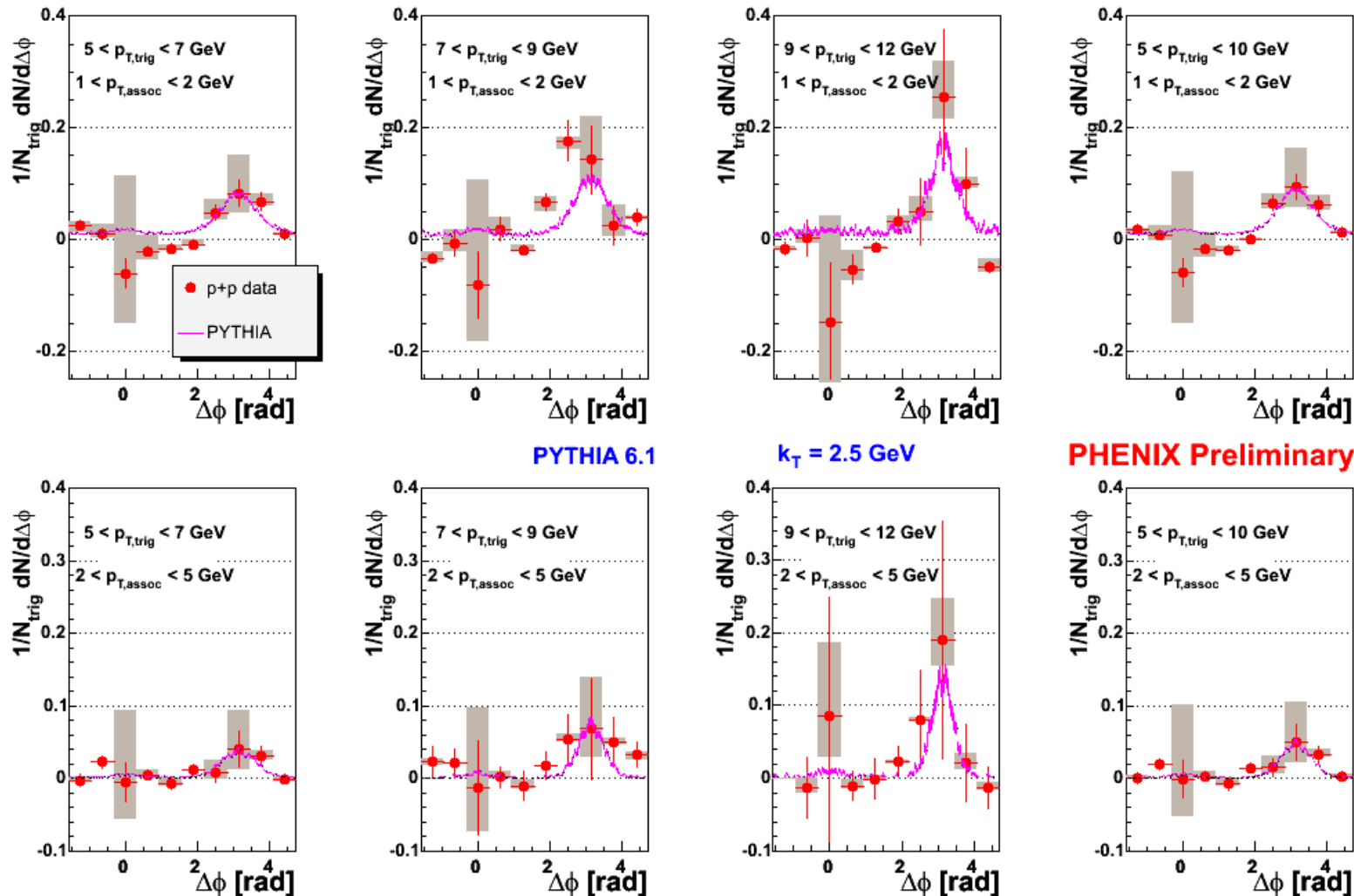
2. decay gamma-hadron correlations from π^0 -hadron correlations.



3. bin by bin subtraction

As a cross-check, near side peak should cancel because direct photons are isolated (at first order). This validates the accuracy of the subtraction.

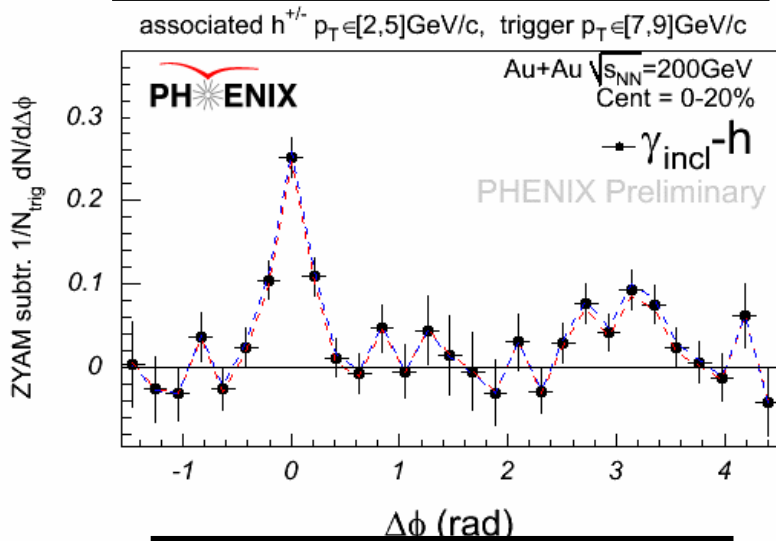
Gamma - jet correlations in p+p



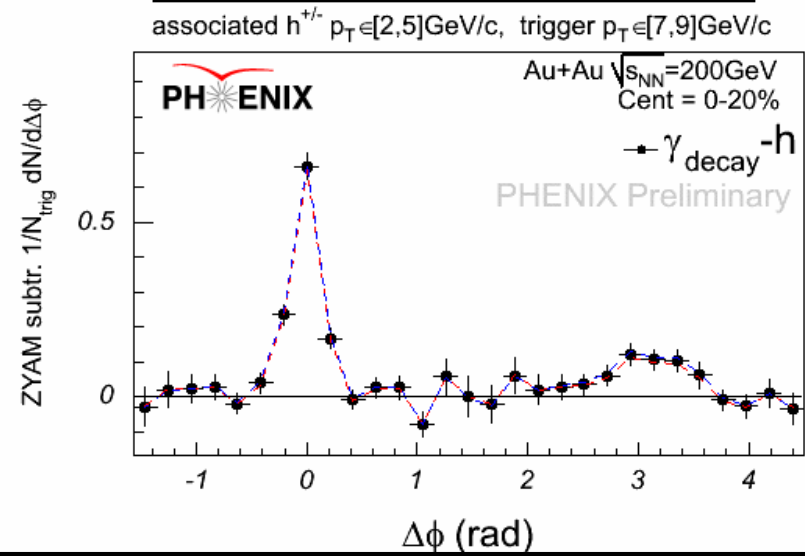
Comparison between p+p direct photon-hadron correlations and pythia. Good agreement achieved although large error bars.

Gamma - jet correlations in Au+Au

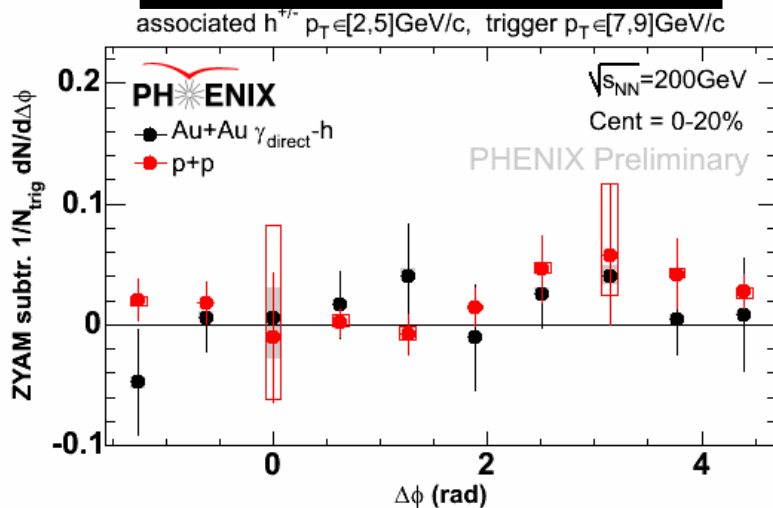
inclusive photon - hadron



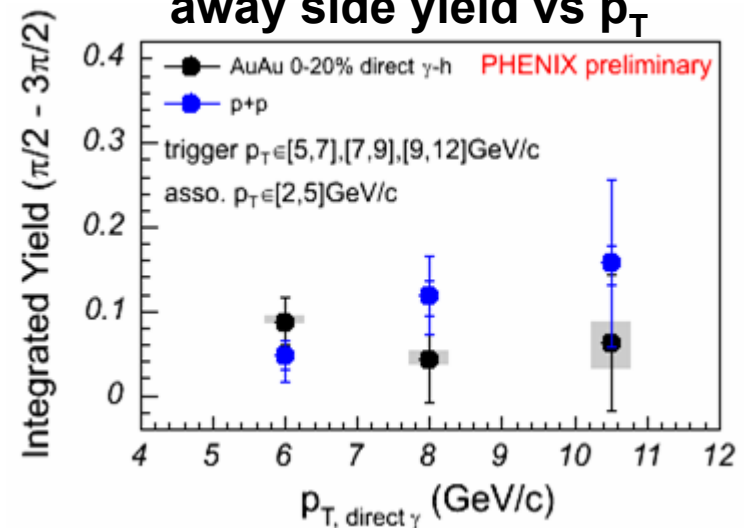
decay photon - hadron



direct photon - hadron



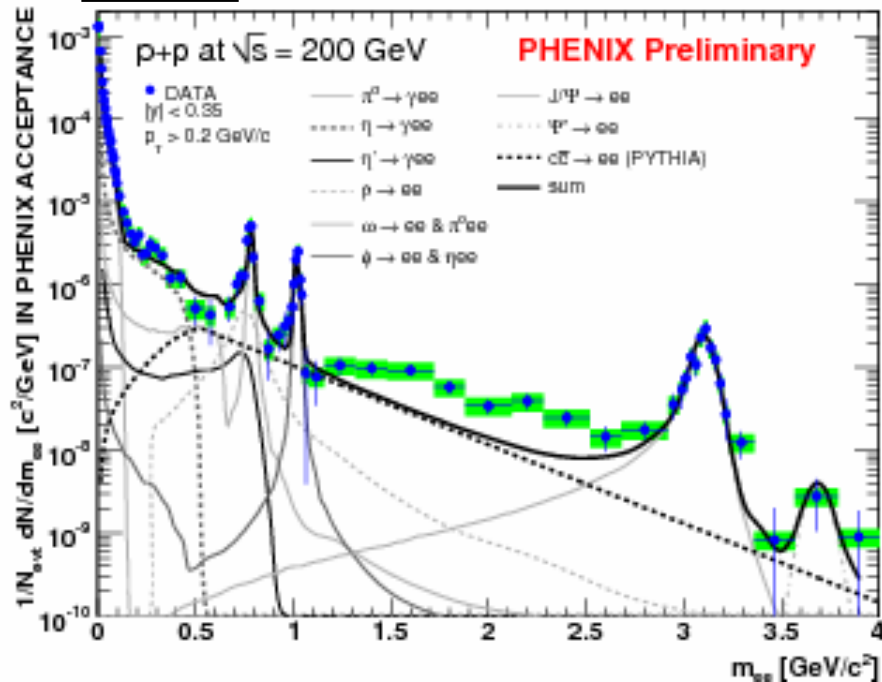
away side yield vs p_T



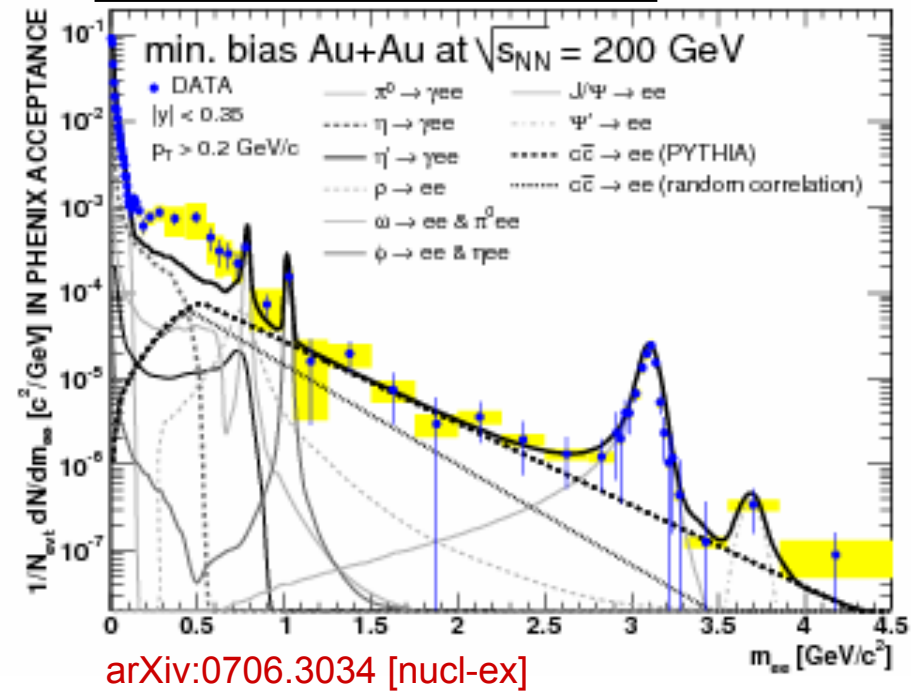
di-lepton continuum and heavy quarkonia

di-electron invariant mass distribution

p+p

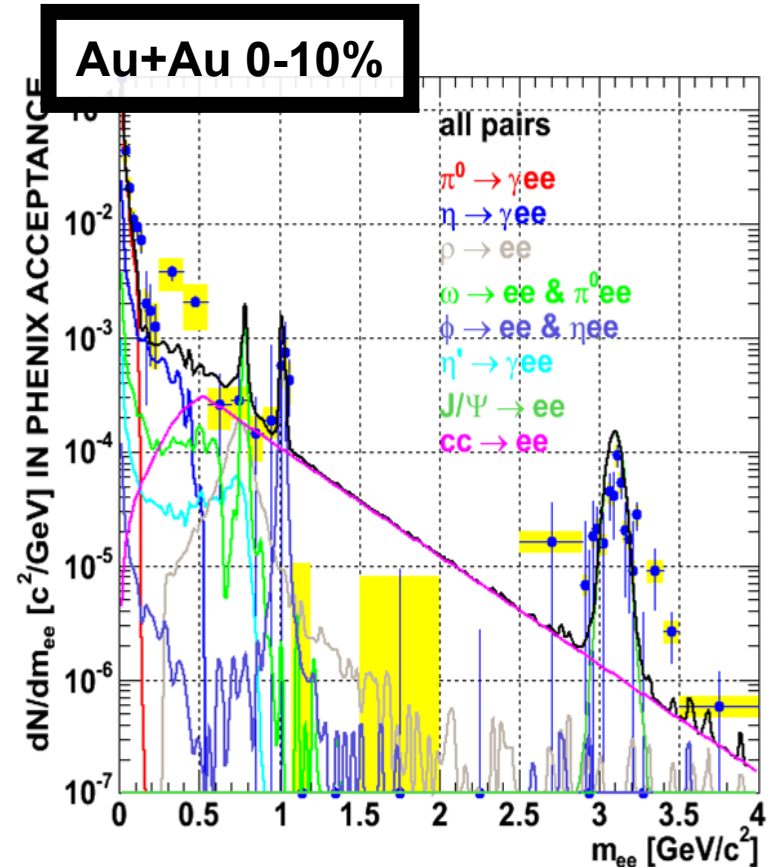
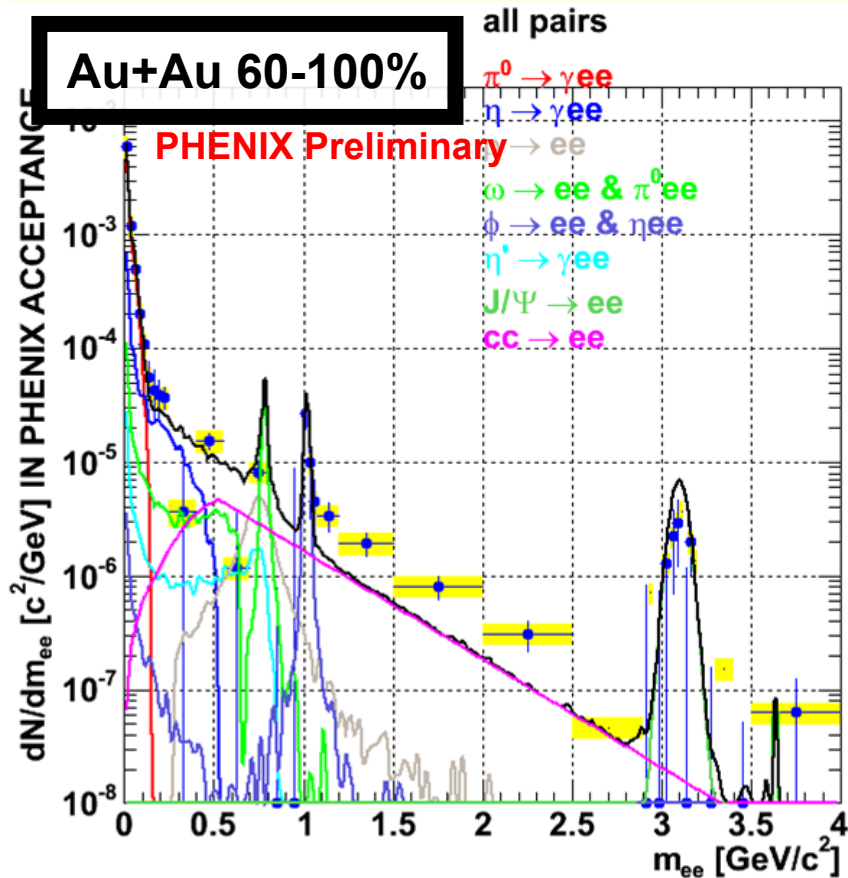


Au+Au minimum bias



An excess is observed at low mass ($m < 1$ GeV/c) in Au+Au minimum bias

di-electron invariant mass distribution centrality dependence

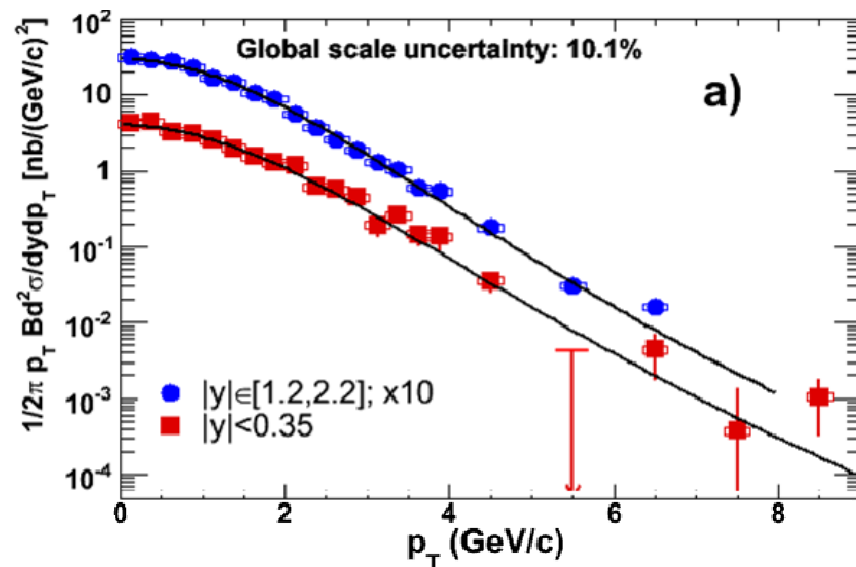
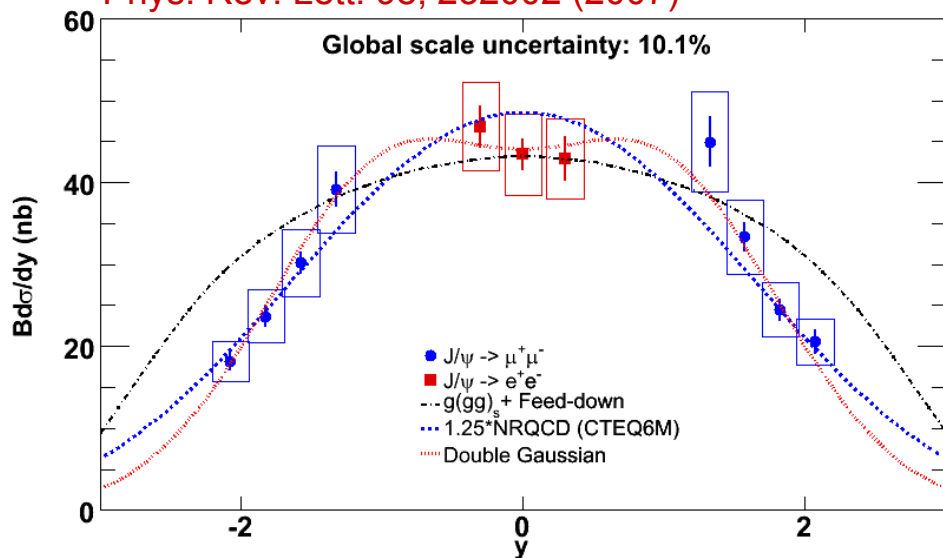


Au+Au peripheral behaves essentially like p+p

Au+Au central: excess at low mass ($m < 1 \text{ GeV}/c$) as for minimum bias.

J/Ψ production in p+p collisions

Phys. Rev. Lett. 98, 232002 (2007)

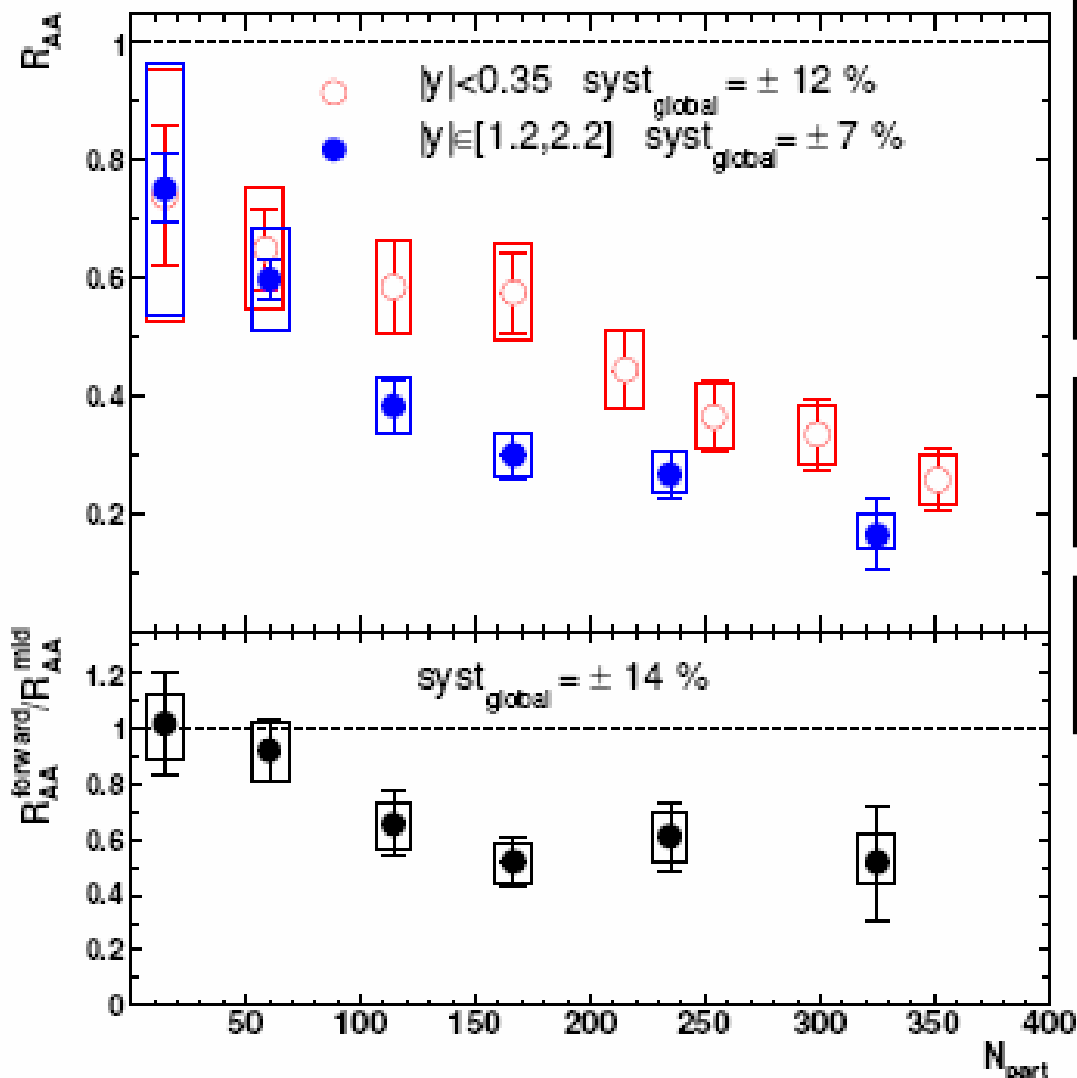


10 times more statistics as previous measurement.

- better constraints on rapidity and p_T spectrum
- better reference for the nuclear modification factor

$$B_{||} \sigma_{J/\Psi}^{pp} = 178 \pm 3(\text{stat}) \pm 53(\text{sys}) \pm 18(\text{norm}) \text{ nb.}$$

J/Ψ R_{AA} Au+Au

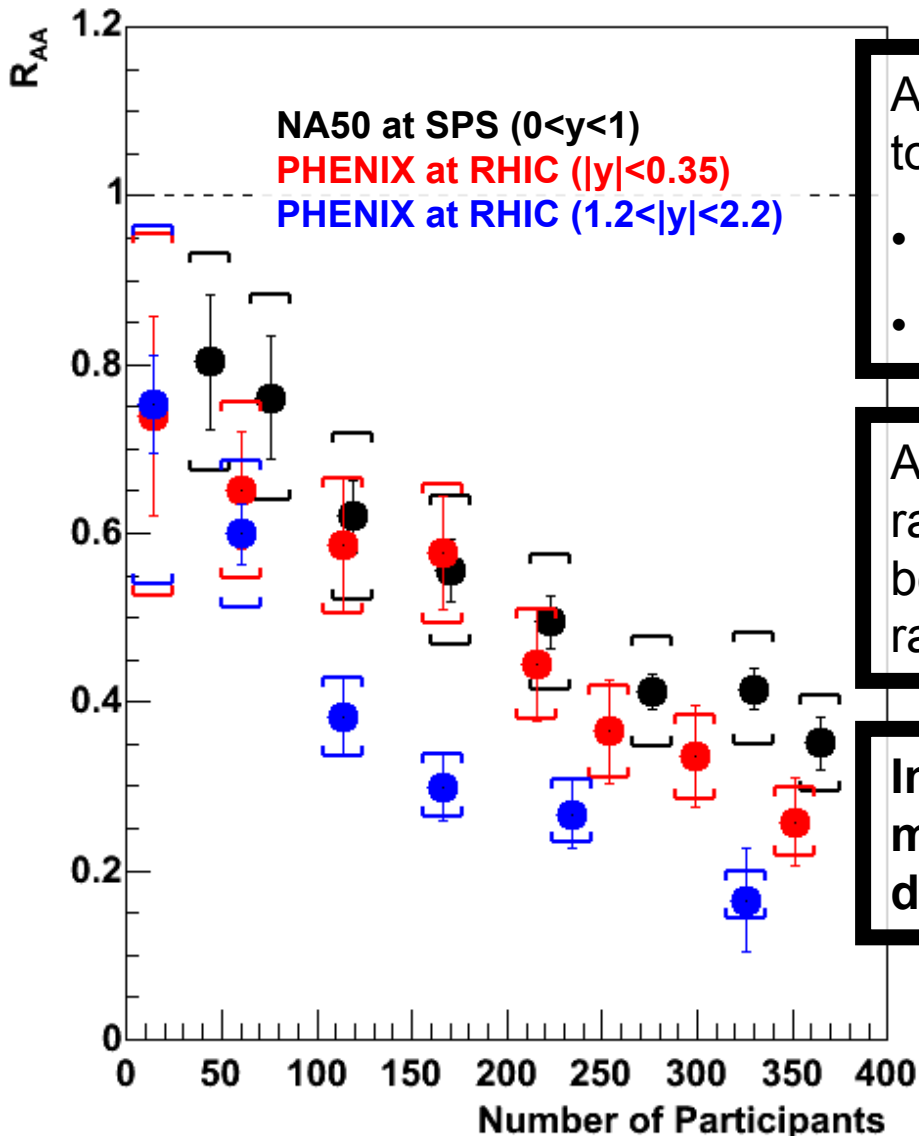


- Vertical bars are statistical and point to point uncorrelated errors
- Boxes are point to point correlated errors

$R_{AA} < 0.3$ for central collisions
 Larger suppression at $|y| > 1.2$

R_{AA} is larger at forward rapidity than at mid rapidity

Comparison to SPS



At mid-rapidity, suppression at RHIC is similar to SPS, but:

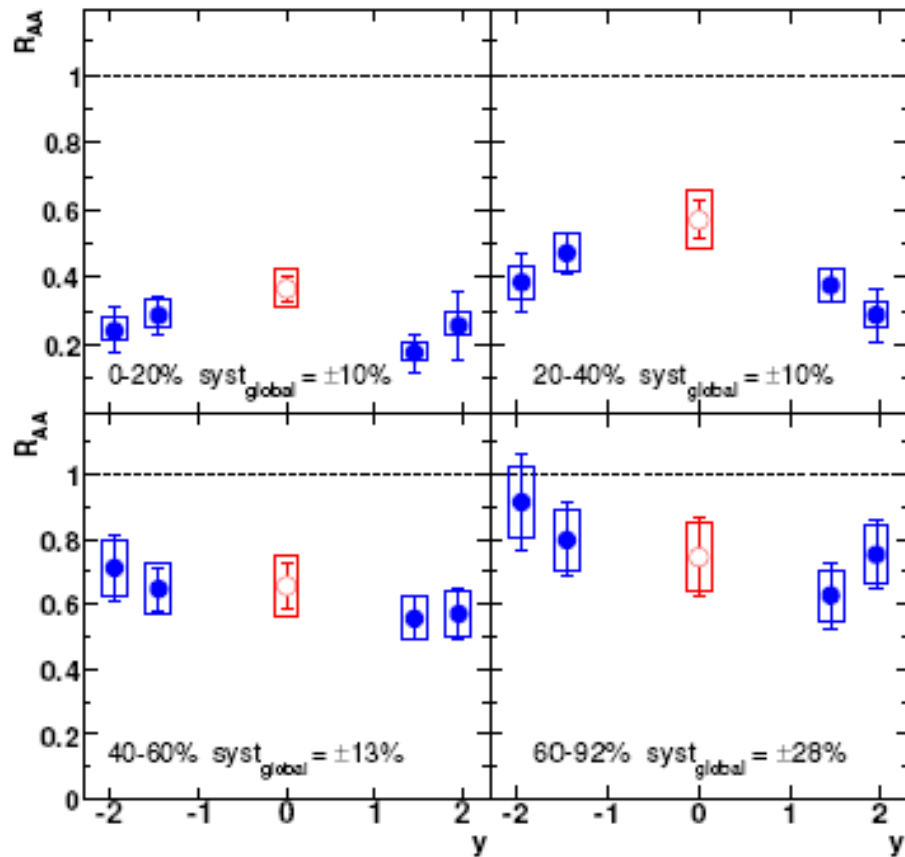
- cold nuclear matter effects may differ
- energy density is larger at RHIC

At RHIC there is more suppression at forward rapidity than at mid rapidity. Unexpected because energy density is larger at mid-rapidity.

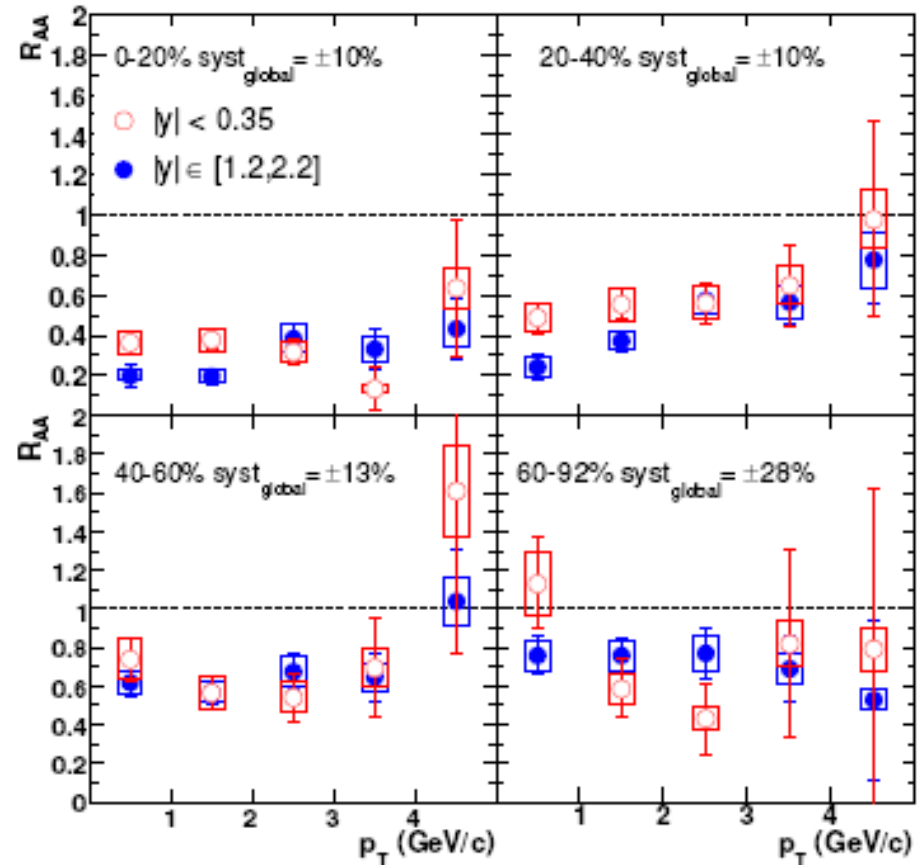
Indications that more complex mechanism must be involved than energy density driven suppression.

R_{AA} vs rapidity and p_T

RAA vs rapidity



RAA vs p_T



And also ...

$J/\Psi R_{AA}$ also measured in Cu+Cu collisions.

Cold nuclear matter effects re-evaluated from d+Au collisions using 2005 p+p data and extrapolated to Au+Au.

4 times more statistics in Au+Au available since 2007 data taking.

Expect a high statistic d+Au data taking in 2008 or 2009.

Conclusions

The matter created in heavy ions collisions at RHIC is dense enough to suppress light hadrons up to very high p_T as well as charmed mesons. Data favor high opacity of the medium, high gluon density and low viscosity.

It strongly affects the jet structure. Data favor Mach cone like deformations (as opposed to deflected jets).

Scaling properties of the elliptic flow indicate that it would form prior to hadronization, meaning that the system is thermalized while still in a partonic phase.

As was originally predicted, J/Ψ is suppressed in the medium, however the picture is more complex than expected. Interplay between cold nuclear matter effects and anomalous suppression is unclear.

Back-up

BNL Facility



length: 3.83 km

Capable of colliding
any nuclear species

Energy:

500 GeV for p-p

200 GeV for Au-Au
(per N-N collision)

protons: Linac → Booster → AGS → RHIC

ions: Tandems → Booster → AGS → RHIC

Collision species and energy

Run	Year	Species	Energy (GeV)	# J/Ψ (ee+μμ)
01	2000	Au+Au	130	0
02	2001/2002	Au+Au	200	13 + 0
		p+p	200	46 + 66
03	2002/2003	d+Au	200	360 + 1660
		p+p	200	130 + 450
04	2003/2004	Au+Au	200	~ 1000 + 5000
		Au+Au	62	13 + 0
05	2004/2005	Cu+Cu	200	~ 1000 + 10000
		Cu+Cu	62	10 + 200
		Cu+Cu	22.5	
		p+p	200	~ 1500 + 10000
06	2006	p+p	200	~ 3000 + 30000
		p+p	62	
		p+p	500	

New detectors

2006

aerogel and time-of-flight system

hadron-blind detector

reaction plane detector

time of flight

forward electromagnetic calorimeter

2006 – 2009

Silicon vertex tracker

muon trigger

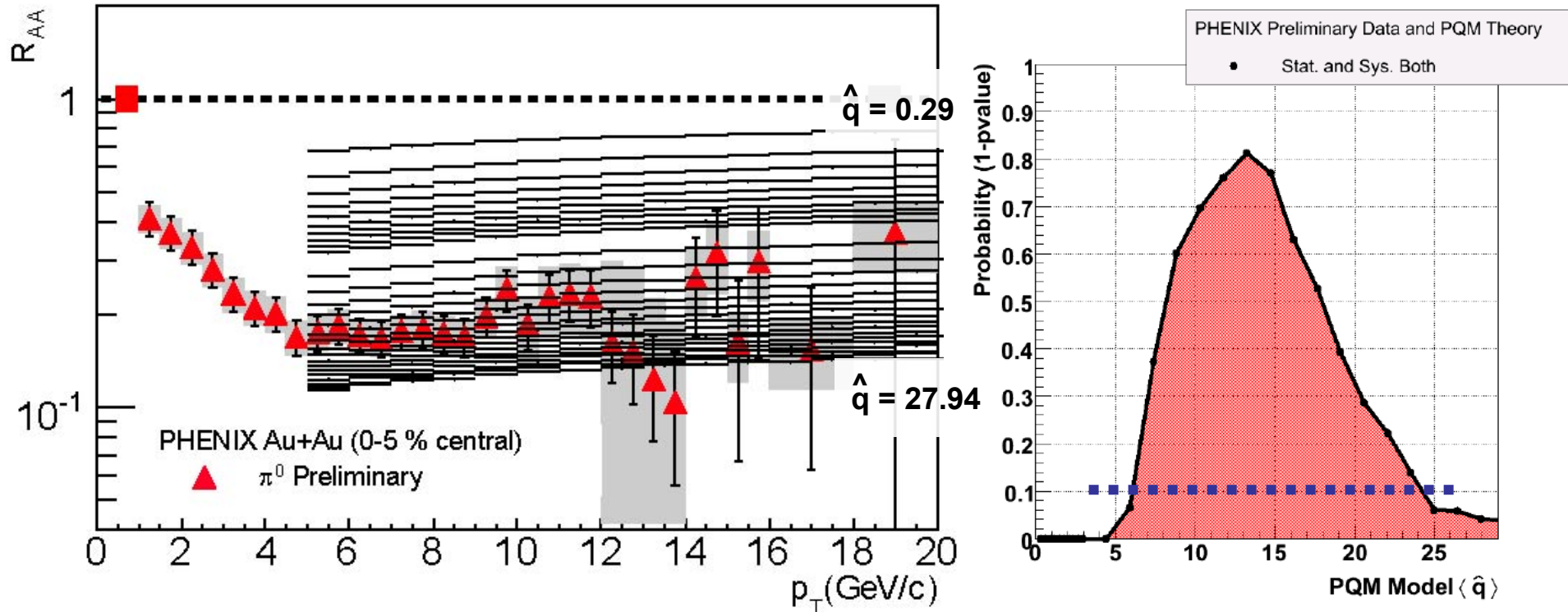
2008 – 2011

forward silicon vertex tracker

nose cone calorimeter

Getting quantitative statements from $\pi^0 R_{AA}$

Comparison of measured $\pi^0 R_{AA}$ to PQM energy loss predictions vs \hat{q}



PQM - C. Loizides hep-ph/0608133v2:

$$6 \leq \hat{q} \leq 24 \text{ GeV}^2/\text{fm}$$

GLV - I. Vitev hep-ph/0603010:

$$1000 \leq dN_g/dy \leq 2000$$

WHDG - W. Horowitz:

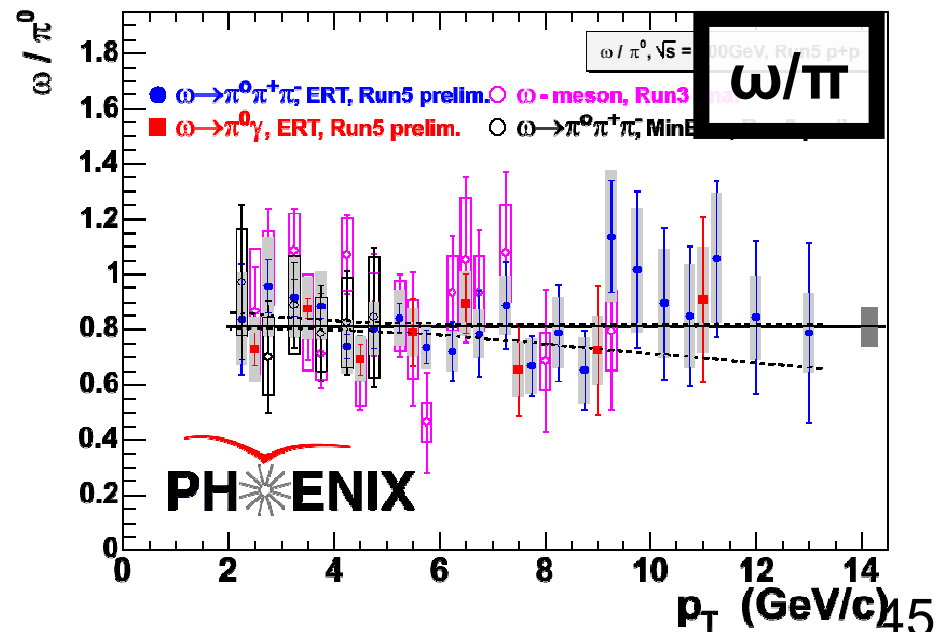
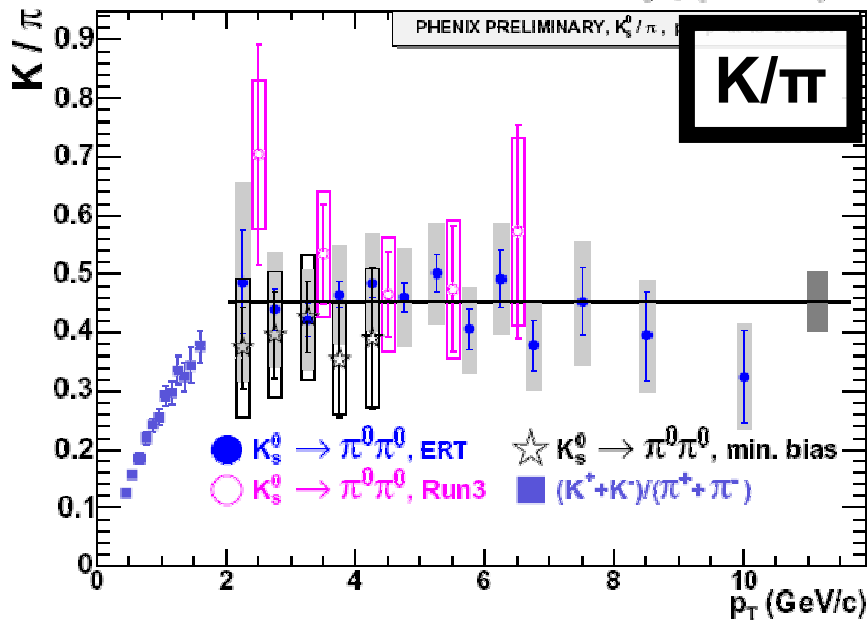
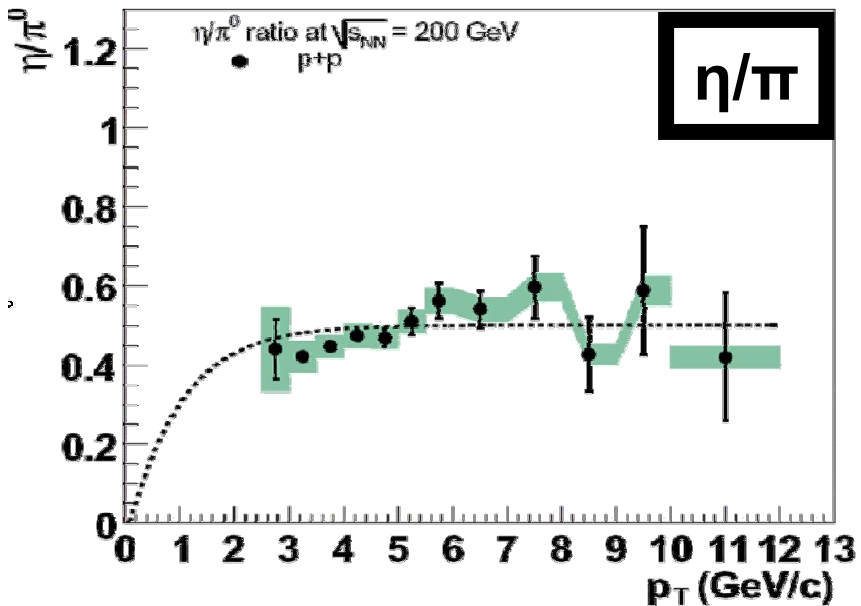
$$600 \leq dN_g/dy \leq 1600$$

Light meson decay channels measured by PHENIX

Light meson resonances

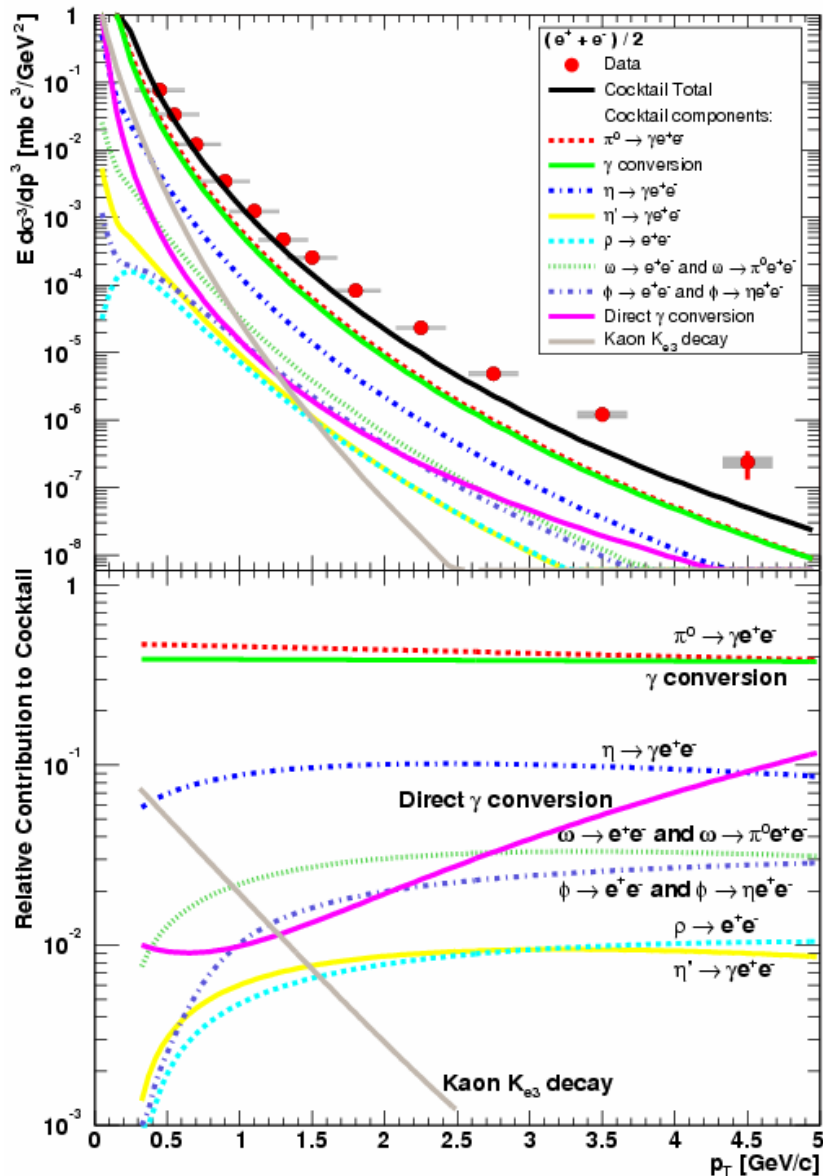
$\phi \rightarrow K^+K^-$	BR = $49.2 \pm 0.7\%$
$\phi \rightarrow e^+e^-$	BR = $2.97 \pm 0.04\%$
$\omega \rightarrow e^+e^-$	BR = $7.18 \pm 0.12\%$
$\omega \rightarrow \pi^0\gamma$	BR = $8.90 \pm 0.25\%$
$\omega \rightarrow \pi^0\pi^+\pi^-$	BR = $89.1 \pm 0.7\%$
$\eta \rightarrow \gamma\gamma$	BR = $39.39 \pm 0.24\%$
$\eta \rightarrow \pi^0\pi^+\pi^-$	BR = $22.68 \pm 0.35\%$
$K^S \rightarrow \pi^0\pi^0$	BR = $30.69 \pm 0.05\%$
K^\pm	using ToF

Light mesons particle ratios



Heavy flavor

Inclusive single electron spectrum and cocktail



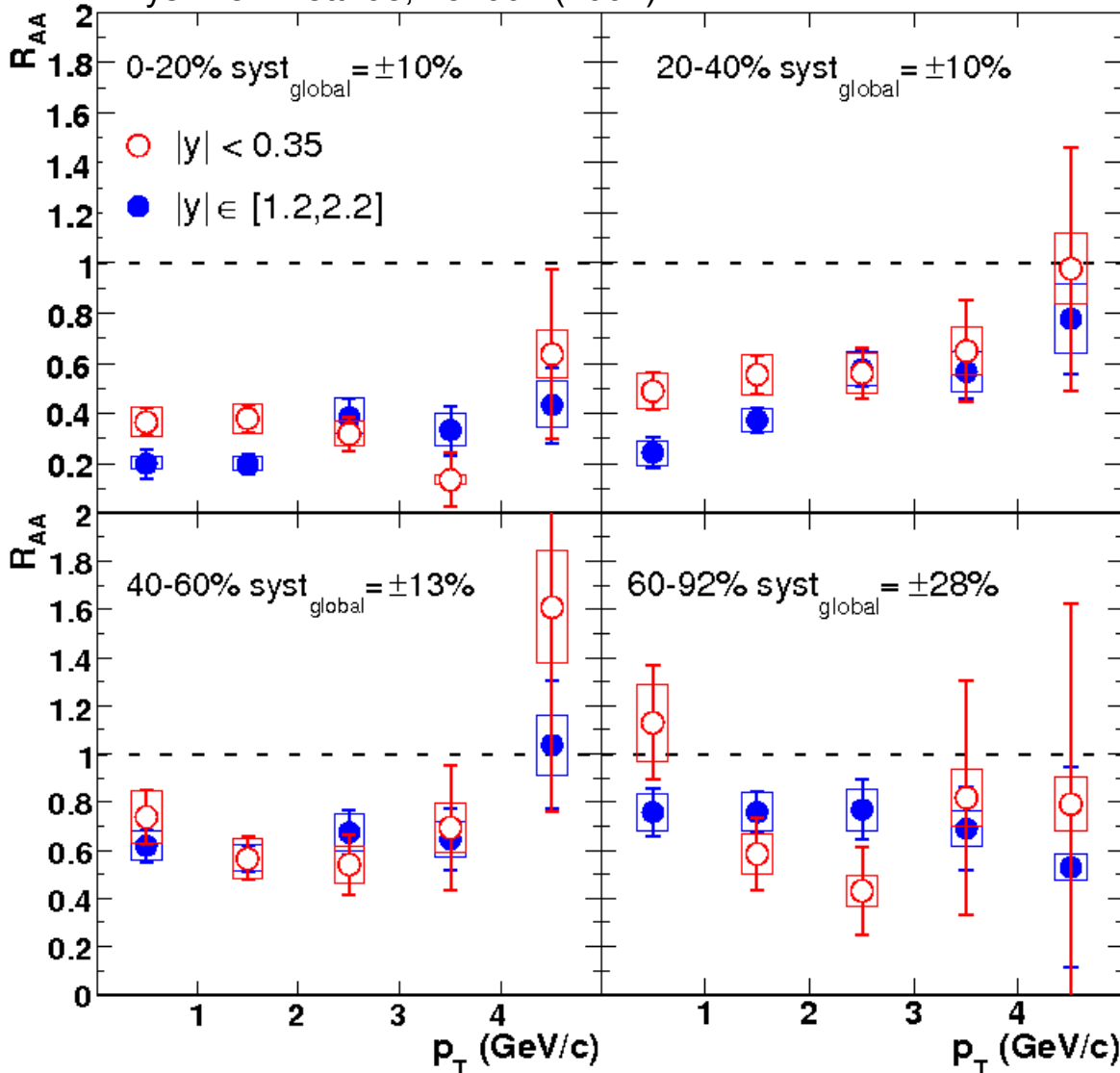
Cocktail method (data driven simulations):

- π contribution based on PHENIX measurements
- γ conversion contribution from material budget
- light meson contributions from lower energy data and m_T scaling from π data

Nuclear modification factor vs p_T in Au+Au

Measurement from 2004 Au+Au (nucl-ex/0611020)

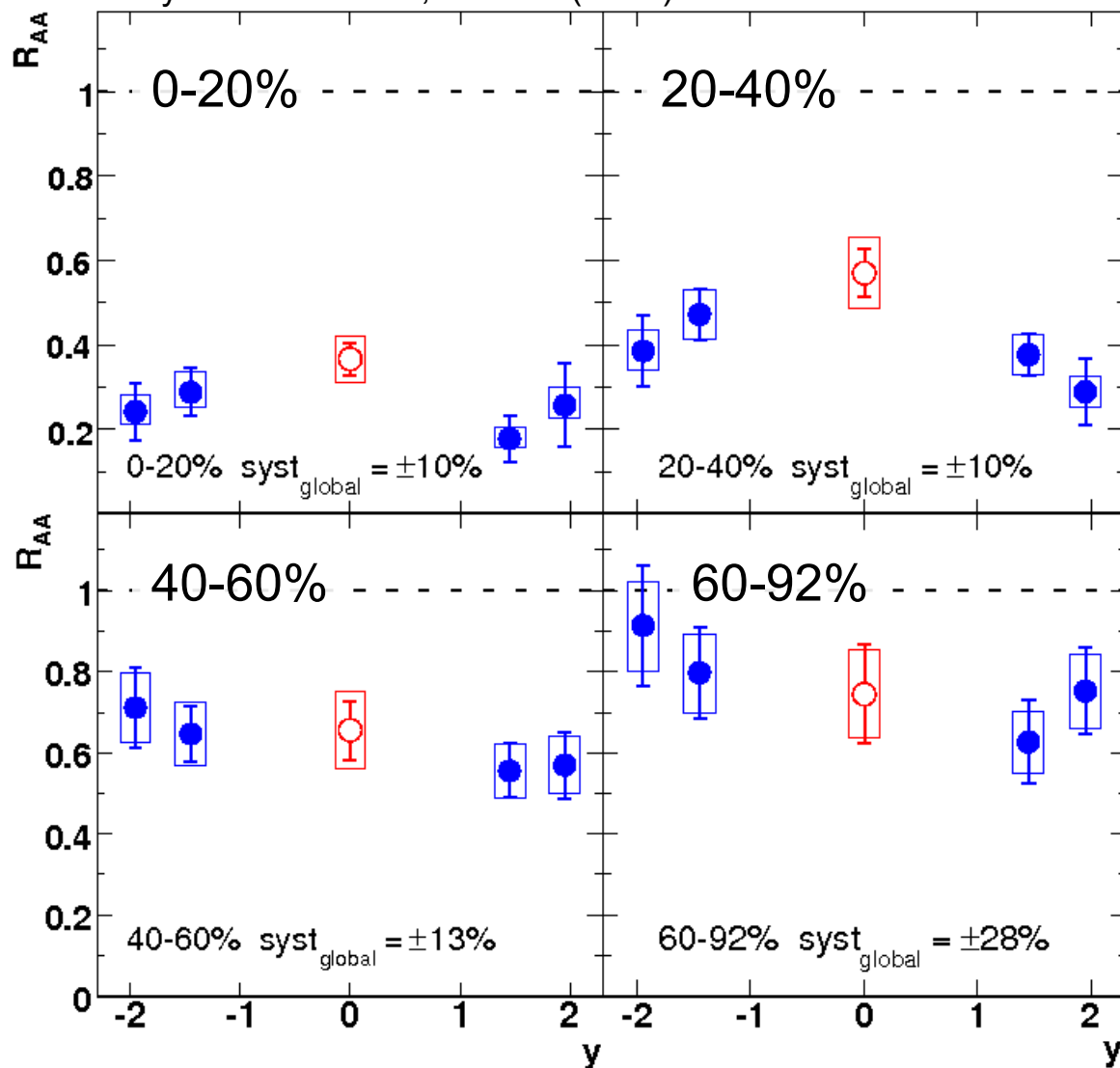
Phys. Rev. Lett. 98, 232001 (2007)



No significant change of the p_T distributions with respect to p+p, but error bars are large

J/Ψ R_{AA} vs rapidity in Au+Au

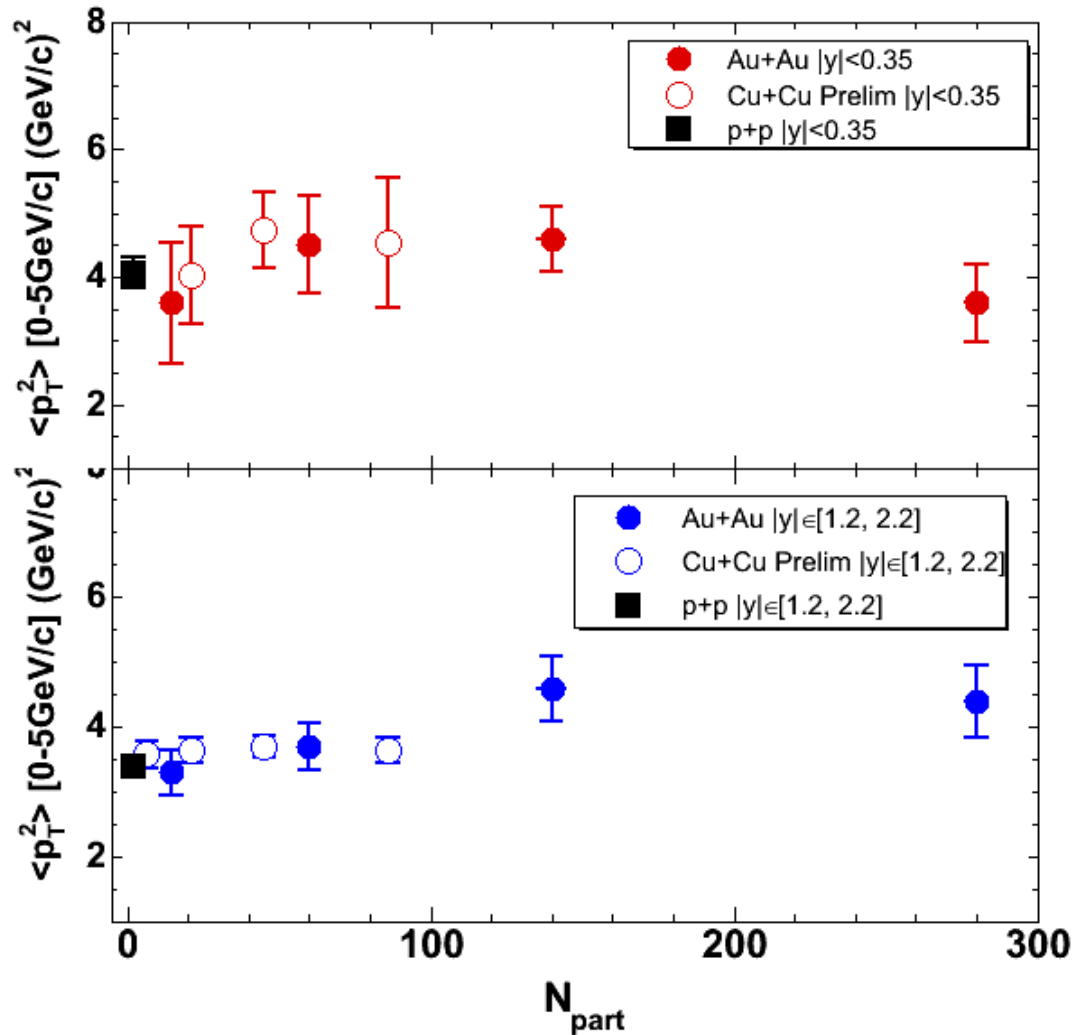
Phys. Rev. Lett. 98, 232001 (2007)



Peripheral collisions:
no modification of the rapidity distribution with respect to p+p collisions

Central collisions:
narrowing of the rapidity distribution

Mean p_T^2 (truncated) vs N_{part}



$\langle p_T^2 \rangle$ (truncated to $0 < p_T < 5 \text{ GeV}/c$) shows no significant variation vs N_{part} for all systems.

Proton spin structure via heavy flavor

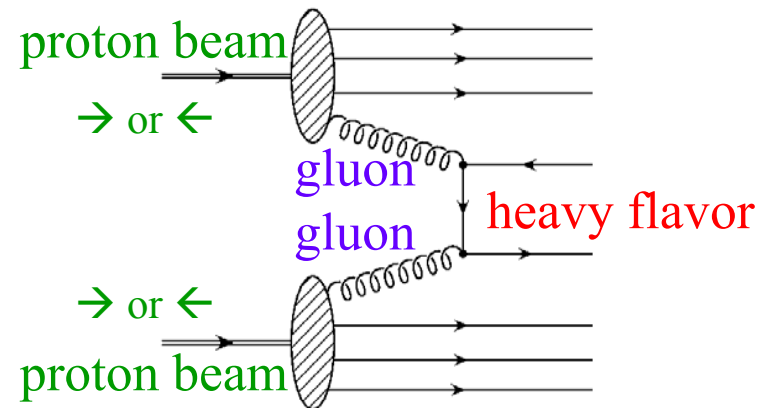
Proton spin structure is probed using longitudinally polarized proton beams. Beam polarization is flipped from bunch to bunch.

Measure particule (here J/Ψ) yields in each configuration, that are sensible to the underlying parton distribution function

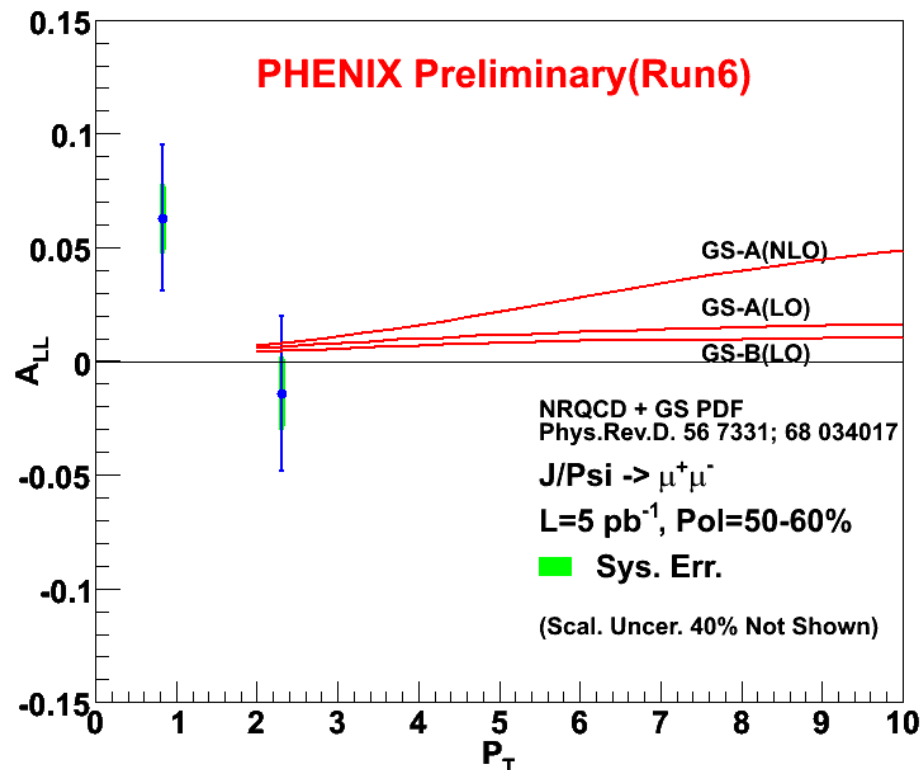
Form asymmetries:

$$A_{LL}^{incl} = \frac{1}{\langle P_B \rangle \langle P_Y \rangle} \frac{N^{++} - R \cdot N^{+-}}{N^{++} + R \cdot N^{+-}}$$

$$A_{LL}^{J/\Psi} = \frac{A_{LL}^{incl} - f_{BG} \cdot A_{LL}^{BG}}{1 - f_{BG}} \approx \frac{\Delta g(x_1)}{g(x_1)} \frac{\Delta g(x_2)}{g(x_2)} a_{LL}^{gg \rightarrow Q\bar{Q}}$$



J/Ψ : $|y| = 1.2-2.4$



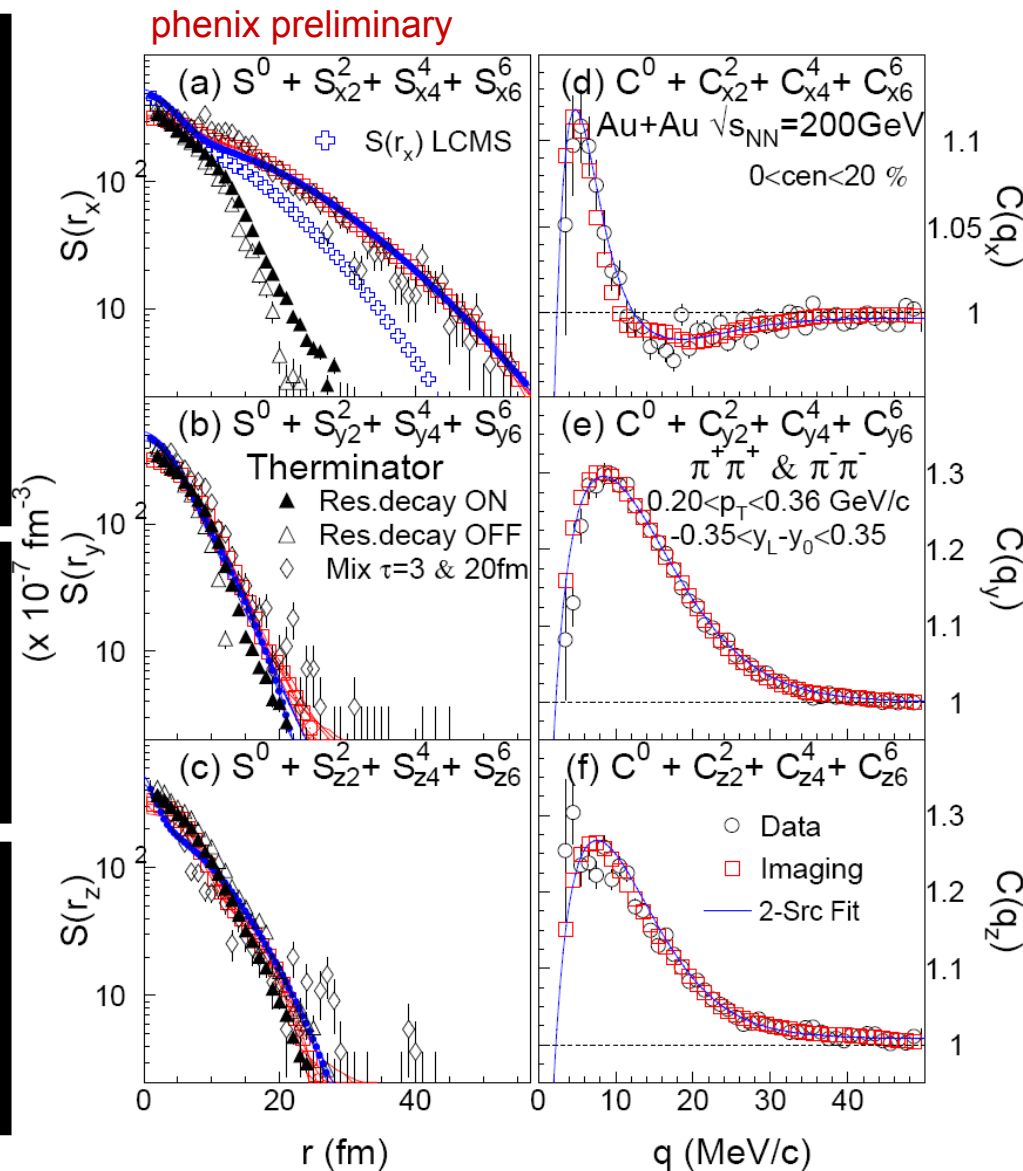
3D two-pions source imaging

Look at 2-pions correlation functions in 3D space; extract 3D cartesian moments of the observed distributions, and from there the 2-pions source functions $S(r)$:

probability to emit a pair of pions at a separation r in the pair rest frame

Source functions describe how pions are produced during hadronization and carry information about the phase transition.

Long range source term along x (parallel to the pair P_T), can be modeled by adding a delayed pion source emission.

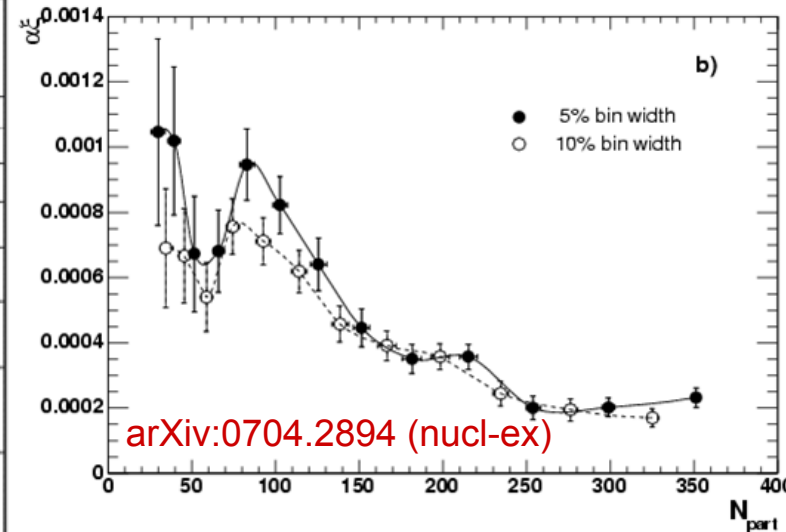
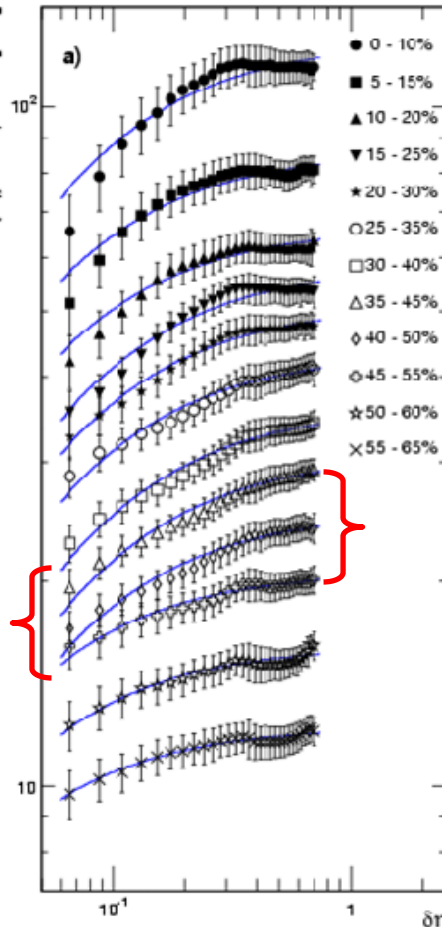
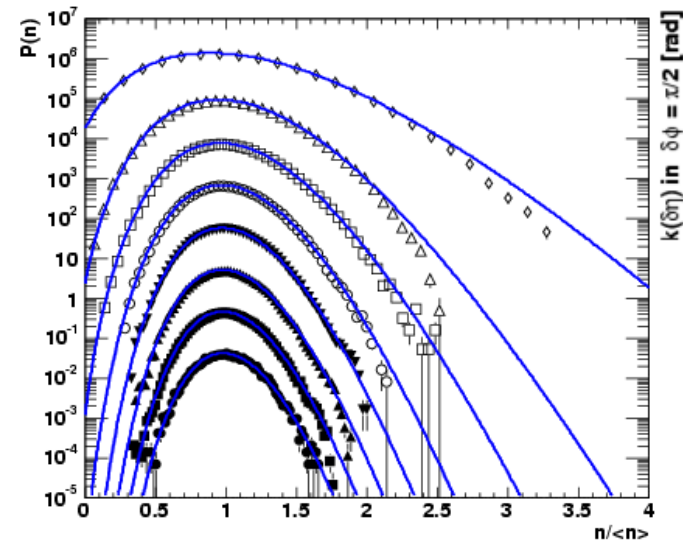


Longitudinal density correlations

1 Fit event/event multiplicity fluctuation vs rapidity domain and centrality with negative binomial distribution (NBD)

2 fit $k(\delta\eta)$, characteristic of the width of the NBD to extract $\alpha\xi$, a parameter monotonically related to the medium **susceptibility**

3 look at $\alpha\xi$ vs N_{part}



The non monotonic behavior $\alpha\xi$ around $N_{\text{part}} \sim 90$ could indicate critical behavior at a phase boundary.